An assessment of western North Pacific ozone photochemistry based on springtime observations from NASA's PEM-West B (1994) and TRACE-P (2001) field studies

D. D. Davis,[1] G. Chen,[1,2] J. H. Crawford,[2] S. Liu,[3] D. Tan,[1] S. T. Sandholm,[1] P. Jing,[1] D. M. Cunnold,[1] B. DiNunno,[1] E. V. Browell,[2] W. B. Grant,[2] M. A. Fenn,[2] B. E. Anderson,[2] J. D. Barrick,[2] G. W. Sachse,[2] S. A. Vay,[2] C. H. Hudgins,[2] M. A. Avery,[2] B. Lefer,[4] R. E. Shetter,[4] B. G. Heikes,[5] D. R. Blake,[6] N. Blake,[6] Y. Kondo,[7] and S. Oltmans[8]

Received 27 November 2002; revised 14 July 2003; accepted 1 August 2003; published 15 November 2003.

[1] The current study provides a comparison of the photochemical environments for two NASA field studies focused on the western North Pacific (PEM-West-B (PWB) and TRACE-P (TP)). These two studies were separated in calendar time by approximately 7 years. Both studies were carried out under springtime conditions, with PWB being launched in 1994 and TP being deployed in 2001 (i.e., 23 February–15 March 1994 and 10 March–15 April 2001, respectively). Because of the 7-year time separation, these two studies presented a unique scientific opportunity to assess whether evidence could be found to support the Department of Energy's projections in 1997 that increases in anthropogenic emissions from East Asia could reach 5%/yr. Such projections would lead one to the conclusion that a significant shift in the atmospheric photochemical properties of the western North Pacific would occur. To the contrary, the findings from this study support the most recent emission inventory data [*Streets et al.*, 2003] in that they show no significant systematic trend involving increases in any O_3 precursor species and no evidence for a significant shift in the level of photochemical activity over the western North Pacific. This conclusion was reached in spite of there being real differences in the concentration levels of some species as well as differences in photochemical activity between PWB and TP. However, nearly all of these differences were shown to be a result of a near 3-week shift in TP's sampling window relative to PWB, thus placing it later in the spring season. The photochemical enhancements seen during TP were most noticeable for latitudes in the range of 25–45°N. Most important among these were increases in $J(O^1D)$, OH, and HO_2 and values for photochemical ozone formation and destruction, all of which were typically two times larger than those calculated for PWB. A comparison of these airborne results with ozonesonde data from four Japanese stations provided further evidence showing that the 3-week shift in the respective sampling windows of PWB and TP was a likely cause for the differences seen in O_3 levels and in photochemical activity between the two airborne studies. *INDEX TERMS:* 0368 Atmospheric Composition and Structure: Troposphere—constituent transport and chemistry; 0345 Atmospheric Composition and Structure: Pollution—urban and regional (0305); 0322 Atmospheric Composition and Structure: Constituent sources and sinks; *KEYWORDS:* TRACE-P, ozone, Pacific Rim

Citation: Davis, D. D., et al., An assessment of western North Pacific ozone photochemistry based on springtime observations from NASA's PEM-West B (1994) and TRACE-P (2001) field studies, *J. Geophys. Res.*, *108*(D21), 8829, doi:10.1029/2002JD003232, 2003.

[1]School of Earth and Atmospheric Sciences, Georgia Institute of Technology, Atlanta, Georgia, USA.
[2]NASA Langley Research Center, Hampton, Virginia, USA.
[3]Institute of Earth Sciences, Academia Sinica, Taipei, Taiwan.
[4]National Center for Atmospheric Research, Boulder, Colorado, USA.
[5]Graduate School of Oceanography, University of Rhode Island, Narragansett, Rhode Island, USA.
[6]Department of Chemistry, University of California at Irvine, Irvine, California, USA.
[7]Research Center for Advanced Science and Technology, University of Tokyo, Tokyo, Japan.
[8]National Oceanographic and Atmospheric Administration, Boulder, Colorado, USA.

Copyright 2003 by the American Geophysical Union.
0148-0227/03/2002JD003232$09.00

1. Introduction

[2] The importance of O_3 in the troposphere has been extensively reviewed in the literature [e.g., *Chameides and Walker*, 1973; *Crutzen*, 1973; *Liu et al.*, 1980; *Logan et al.*, 1981]. Chief among them is its role as a major primary source of HO_x radicals (OH and HO_2). Indirectly, therefore, O_3 is among the most critical chemical agents in the atmosphere leading to the removal of a wide range of atmospheric trace gases [e.g., *Logan et al.*, 1981; *Chameides and Davis*, 1982; *Thompson and Cicerone*, 1986; *Berresheim et al.*, 1995]. On the other hand, it is also now well documented that it can inadvertently be overproduced from expanding industrial emissions, power generation, and transportation needs. Uncontrolled, this enhanced production can lead to elevated O_3 levels that result in human health problems, cause extensive crop damage, and possibly lead to climate effects. Thus a comprehensive understanding of the processes that control O_3 continues to be one of the highest priorities in tropospheric chemistry, locally, regionally, and globally.

[3] On both the regional and global scales, it is now understood that air pollution recognizes no borders. Ozone chemical precursors generated in one country are readily transported to the air space over adjacent countries, the net effect often being the generation of elevated levels of O_3 in these countries. In this country, released O_3 precursors frequently end up in the Atlantic, some of which reach Europe. Similarly, East Asian Pacific Rim emissions penetrate the pristine North Pacific and, on occasion, reach mainland USA [*Jacob et al.*, 1999; *Jaffe et al.*, 1999; *Newell and Evans*, 2000]. In the current study, the focus will be on the latter region.

[4] As part of NASA's Global Tropospheric Experiment (GTE), a major effort has been made during the decade of the 1990s to study the atmospheric chemistry of the Pacific. The rationale has been that the Pacific is among the few global regions left that is relatively clean. Thus it defines one of the few regions left where benchmark measurements of trace gas concentrations can be recorded and their sources and sinks evaluated. Such observations can serve as a reference point for future studies, thereby providing a basis for quantifying the rate at which chemical change is occurring in the atmosphere. One of the early Pacific GTE field studies designed to carry out this cited objective was that labeled: Pacific Exploratory Mission-West B (PEM-West B, hereafter PWB). This study took place in 1994 and had as a centrally important component of its sampling strategy examining air parcels over the western North Pacific Ocean. Of particular significance was the investigation of air parcels influenced by the contiguous Pacific Rim countries of Japan, Korea, and China. At that time, East Asia was recognized as one of the fastest growing regions in the world in terms of rate of industrialization. Reflecting this, in 1997 the U.S. Department of Energy projected an energy growth rate for East Asia of 5% per year; and since the combustion of fossil fuel provides the major source of energy for this region, it follows that both sulfur and nitrogen oxide emissions should have steadily increased over the last several years. Countering this earlier projected expansion in energy consumption, however, has been the onset of a significant economic slowdown in East Asia. This slow down emerged as a full-blown recession by the late 1990s. As a result, the most recent emission inventories for the Pacific Rim actually suggest that the growth rate in such critical pollutant species as SO_2 and NO_x may be no more than 10 to 15% [*Streets et al.*, 2003].

[5] The current study examines the above emission inventory conclusion by taking advantage of the most recently generated NASA GTE chemical data base for the western North Pacific, the Transport and Chemical Evolution over the Pacific program (TRACE-P, labeled hereafter as TP). The latter study, like PWB, was deployed in the spring, but it took place in the year 2001. As a result, it has provided a unique scientific opportunity to look at the western North Pacific and Pacific Rim region from the perspective of evaluating the chemical change occurring over a 7-year period. Specifically, this study has focused on photochemical change. It therefore examines the trends in ozone precursors, ozone itself, and the overall level of photochemical activity.

2. Observational Data Base

[6] The observational data base used here is that provided by NASA's PWB and TP programs plus ozonesonde data from four Japanese stations. As in all such studies using airborne field data, an assessment of a trend when comparing the results from one study with another, one assumes that the field sampling itself has been sufficiently comprehensive as to be ''representative'' of the time period and atmospheric domain sampled. Given the soundness of this assumption, it then becomes possible to look at the differences in the levels of species and parameters as an indication of a trend in these over time. That anomalous behavior might have occurred involving one or more natural cycles, thereby influencing the concentration levels of the species being measured during the two field programs, is always possible. Thus some measure of such perturbations needs to be considered in assessing long-term trends. One way of achieving this is having available continuous long-term records of at least one critical species that overlap the time period of the airborne field studies. For the current study this has been primarily achieved through our examining Japanese ozonesonde data. Details concerning each data source are provided below.

2.1. Airborne NASA Data

[7] The airborne data recorded during PWB was collected only on the NASA DC-8 aircraft. For TP, both the DC-8 and P-3B were available for data collection. This increase resulted in a TP data base that was roughly twice as large as that for PWB. To define the region of comparison in the North Pacific, an assessment was first made of the data distribution as a function of latitude and longitude. This was followed by an examination of the magnitudes of several pollution parameters. The latter effort then provided a basis for defining the boundary between areas representative of marine-background conditions versus those more strongly influenced by Asian outflow. From this, a ''working'' data base was defined which covered the latitude range of 5°N to 45°N. For the latitude range of 5° to 25°N, the western boundary approximated the Asian coast and the eastern boundary was 145°E. (The authors note that the location of

the ITCZ during TP/PWB generally ranged from 5°S to 5°N, but overall was quite weak during both studies). For latitudes of 25° to 45°N, the western boundary was also approximated by the Asian coast, but the eastern boundary extended out to 155°E. As discussed in greater detail in section 4.1, the division of the airborne data set into two domains, with the division coming at 25°N, was predicated on there being significant concentration gradients in several trace gas species near 25°N. In general, higher values were found in the more northerly domain. However, the data in this high latitude zone were further restricted in altitude so as not to include stratospheric observations, e.g., $\leq$8 km. Although the tropopause height was actually higher than this at 25°N, it fell off rather rapidly with increasing latitude. Thus, at altitudes above 8 km, it was not uncommon to find a mixture of stratospheric and tropospheric air. In the current study a more conservative approach has been taken in that for the latitude range of 25–45°N only data recorded at 8 km or below have been analyzed.

[8] As discussed in detail in section 4.2, a critical aspect of the current comparison of the PWB and TP airborne studies has involved the exact calendar timing of each. Although both were carried out during springtime, the center of gravity in calendar time for each sampling window was different. For example, the TP window was centered almost 3 weeks later than PWB. For PWB, it was 6 March 1994, with the earliest observations coming on 23 February and the latest on 15 March. For TP, the center was 25 March 2001, with the earliest observations being recorded on 10 March and the latest on 15 April.

[9] Some of the plots that have been generated to facilitate the comparison of PWB data with that from TP have been constructed in the form of altitude/latitude grid plots. In these cases median values were estimated for each parameter, and it was these that defined the value placed in each grid box. Similarly, the altitude versus concentration plots were also based on estimates of the median value for each altitude range. Medians were estimated from appropriately binned data taken from the 30-s merged data set for PWB and the 1-min merged data set for TP.

[10] A detailed description (e.g., sensitivity, resolution, LOD, and detection principle) of each instrument used to measure the critical species CO, H_2O, O_3, NO, CH_4, and NMHC's has been provided by individual investigators in the TP AGU "Special Issue" and/or in the PWB "Overview" [*Hoell et al.*, 1997]. Of particular significance, as related to the NO observations, is the fact that the same instrument types (Laser-Induced Fluorescence and Chemiluminescence) and the same experimental groups were involved in both field studies. Additionally, these two systems have previously undergone a successful formal intercomparison down to the 10 pptv level [e.g., see *Crawford et al.*, 1997a].

2.2. Ozonesonde Data

[11] The ozonesonde data used in this study to examine the long-term and seasonal trends in Pacific Rim O_3 were those obtained from four Japanese ozonesonde stations administered by the Japanese Meteorological Agency. The data were recorded at Naha (26.2°N, 127.7°E), Kagoshima (31.6°N, 130.5°E), Tateno/Tsukuba (36.1°N, 140.1°E), and Sapporo (43.1°N, 141.3°E). The ozonesondes employed by these stations used sensors that were based on the carbon-iodine measuring method. The temporal coverage of the Japanese ozonesonde data was from 1991 to 2001. The vertical resolution for this data was ~100 m. For the current study, median values were derived from the observational ozonesonde data using a 1-km bin size, and a temporal integration time which ranged from one month to multiple years, depending on the application.

3. Model Description

[12] The model used in the present study was our standard GIT/LaRC time-dependent box model (TDM) which has been employed in numerous previous studies [e.g., *Davis et al.*, 1996; *Crawford et al.*, 1997a; *Crawford et al.*, 1999; *Chen et al.*, 2001]. All relevant reactions now being used in the model have recently been listed in the work of *Crawford et al.* [1999]. In our standard model runs output species are integrated in time until their diurnal cycles reach a quasi-steady state, i.e., concentration profiles matching the previous day's pattern. The rate constants used in this model which encompass all relevant HO_x-NO_x-CH_4 chemistry have been primarily taken from *DeMore et al.* [1997] with updates in values reflecting still more recent changes. The one major exception to the above statement involves the photolysis rate for O_3. Its value has been taken from *Talukdar et al.* [1998]. The model's NMHC chemistry is that based on the condensed version of the *Lurmann et al.* [1986] model with updates in rate coefficients as reflected in the work of *Atkinson et al.* [1992]. Modifications to the Lurman model include explicit chemistry for some previously "lumped" family hydrocarbons (e.g., acetone, propane, and benzene), and added reactions to reflect remote background conditions where NO_x levels are low. The latter change, in particular, allowed for the formation and recycling of organic peroxides. The one sigma error generated from the combined uncertainties in the reaction rate constants (i.e., based on Monte Carlo calculations) has been estimated to be $\leq$30% (1-sigma error) for key species such as OH and HO_2 as well as for the photochemical quantities $F(O_3)$, $D(O_3)$, and $P(O_3)$) [*Davis et al.*, 1993].

[13] The current version of our model has been used in the analysis of both the PWB and TP data sets. Thus any differences in model output are due to differences in the observational data recorded during these two programs. Model runs were typically constrained by observational data for O_3, NO, dew point, CO, and NMHCs. However, for TP they were also constrained by observed values for CH_3OOH and H_2O_2, when available. This occurred ~35% of the time. Independent tests revealed that the additional constraint imposed on the model by using the peroxide data typically had less than a 5% effect on the predicted levels of HO_x. Only sampling periods having NO levels corresponding to solar zenith angles of less than 70° were analyzed since NO_2 data were frequently unavailable. The NO observations were used to generate a total short-lived nitrogen oxide quantity, NOy', which was defined as the sum of NO, NO_2, N O_3, N_2O_5, HONO, and HO_2NO_2. The partitioning between these species was dictated by the model's photochemical mechanism [*Crawford et al.*, 1999]. Ozone column densities, used in the evaluation of all J-values, were estimated from TOMS satellite data recorded

during each respective field study at the latitude/longitude and time of the observation. J values were evaluated using the NCAR Tropospheric Ultraviolet-Visible (TUV) radiative transfer code [*Madronich and Flocke*, 1998]. These model-generated J-values were further adjusted for cloud effects based on the independently derived J-values measured during the field study. The latter measuring systems consisted of either a filter radiometer or a spectro-radiometer instrument [e.g., *Crawford et al.*, 1997a; *Lefer et al.*, 2003]. All final model output products were converted to 24-hour averaged values. As recently shown by *Davis et al.* [2001], in an extensive comparison of field observed OH values with those generated from the current GIT/LaRC TDM model (e.g., data from PEM-Tropics A and B), the general agreement between model products and observations has typically been within a factor of 1.5. A comparison of model generated J values with those derived from the spectro-radiometer data have been previously carried out and shown to typically be within 5–15%.

[14] In addition to the basic photochemical model output (e.g., OH, HO_2, CH_3O_2, RO_2, CH_2O, etc.), diurnal averaged values were also generated for photochemical O_3 formation, destruction, and net tendency (i.e., $F(O_3)$, $D(O_3)$, and $P(O_3)$). These output parameters have been previously defined [e.g., see *Chameides et al.*, 1987; *Davis et al.*, 1996; *Crawford et al.*, 1997b] and are here represented in the form of equations (1)–(3).

$$F(O_3) = k4[NO][HO_2] + k5[NO][CH_3O_2] + k6[NO][RO_2] \quad (1)$$

$$D(O_3) = k3[O1D][H_2O] + k8[O_3][HO_2] + k7[O_3][OH] + (k10[NO][O_3]k12[NO_2][OH]/\{k11 \cdot [NO_2 + k12[NO_2][OH]\}) \quad (2)$$

$$P(O_3) = F(O_3) - D(O_3) \quad (3)$$

Key reactions involved in this photochemistry are those listed in Table 1. The authors note that the last term in equation (2), involving reactions R12 and R11, is usually insignificant except in those cases where NO_x levels exceed 500 pptv.

4. Results and Discussion

[15] As cited earlier in the text, the focus of this study is that of evaluating photochemical change in the atmosphere over the northwestern North-Pacific. The time period over which this change is being assessed is that defined by the 7 years separating the NASA GTE PWB and TP field studies. The approach taken has involved looking first at the trends in ozone precursor species (e.g., NMHCs, CO, H_2O, and NO), and then ozone, and finally at the critical photochemical model products $J(O^1D)$, OH, HO_2, $F(O_3)$, $D(O_3)$, and $P(O_3)$. The results have then been analyzed from two different perspectives: (1) in terms of increases in pollution emissions over the 7-year period between field campaigns and (2) in terms of the 3-week shift that occurred in the sampling windows between the two programs. The conclusions derived from the airborne PWB/TP data were then further tested by comparing them against the results derived from an examination of 10 years of East Asia ozonesonde data.

Table 1. Key Reactions in Ozone Photochemistry

Reaction	
(R1)	$O_3 + h\nu \rightarrow O(^1D) + O_2$
(R2)	$O(^3P) + O_2 \rightarrow O_3)$
(R3)	$O(^1D) + H_2O \rightarrow 2OH$
(R4)	$HO_2 + NO \rightarrow NO_2 + OH$
(R5)	$CH_3O_2 + NO \rightarrow NO_2 + CH_3O$
(R6)	$RO_2 + NO \rightarrow NO_2 + RO$
(R7)	$O_3 + OH \rightarrow HO_2 + O_2$
(R8)	$O_3 + HO_2 \rightarrow OH + 2O_2$
(R9)	$HO_2 + HO_2 \rightarrow H_2O_2 + O_2$
(R10)	$NO + O_3 \rightarrow NO_2 + O_2$
(R11)	$NO_2 + h\nu \rightarrow NO + O(^3P)$
(R12)	$NO_2 + OH + M \rightarrow HNO_3$

4.1. Airborne Ozone Precursor Profiles

[16] The first precursor species examined here is the NMHC, C_3H_8. C_3H_8 can be viewed as a representative member of a NMHC family having moderate reactivity toward OH, e.g. see Table 2. In this case the altitude/concentration plots shown in Figure 1a reveal that the C_3H_8 distribution for both field studies has a well-defined spatial trend. (In these plots the C_3H_8 data have been binned in 1-km increments for both 5–25°N and 25–45°N)) Of particular interest, however, is the apparent long term temporal trend that is evident. Over the time period of 1994 to 2001 (e.g., PWB versus TP), decreasing levels of C_3H_8 can be seen. This trend is especially noticeable for latitudes >25°N where the difference ranges from a factor of 1.5 to 2.0, PWB being higher. This clearly is in conflict with that suggested by the latest emission inventory data which would point to a likely increase of 10–14% for moderately reactive NMHCs [*Streets et al.*, 2003].

[17] If a still more reactive NMHC species is examined, C_3H_6 (see Table 2), the difference is found to be even more dramatic. For this species the concentration found during PWB for the 25–45°N zone exceeded that for TP by factors ranging from 3 to 15. Although some of this difference can be understood in terms of the higher reactivity of C_3H_6 toward OH, other factors could serve to complicate this interpretation. These could include the seasonal trends in natural bioemissions and/or biomass burning. Even the accuracy of the C_3H_6 measurement themselves would want to be listed as a possible source of the difference seen between PWB and TP. Most likely, however, for a very short-lived species like C_3H_6, the transport time from the point of origin to the actual sampling location also plays a major role in dictating the magnitude of the observed shift between studies. Overall, though, there can be little doubt that these reactive NMHCs are revealing the presences of a strong seasonal photochemical trend which manifests itself in terms of concentration differences between the two studies, with the earlier study having the higher levels.

[18] When a trace gas species is selected for comparison that has a lower OH reactivity than C_3H_8, the above trend either weakens or totally disappears. Examples of the latter type can be found in the distributions of C_2H_2 and CO. For C_2H_2 (Figure 1b), which according to Table 2 is 1.5 times less reactive than C_3H_8, PWB levels are seen as still being slightly higher than those in TP; but the difference has

Table 2. Comparison of NMHC Lifetimes Between PWB and TP Sampling Windows

	T = 298 K, P = 1000 mb		T = 260 K, P = 500 mb	
Compound (X)	K (X + OH)	Lifetime (d)	K (X + OH)	Lifetime (d)
		TRACE-P		
C_2H_2	7.46E-13	19.4[a]	5.62E-13	25.7[a]
C_3H_8	1.09E-12	13.3[a]	7.90E-13	18.3[a]
C_3H_6	2.63E-11	0.5[a]	3.37E-11	0.4[a]
CO	2.39E-13	60.6[a]	1.94E-13	74.4[a]
		PEM-West B		
C_2H_2	7.46E-13	38.8[b]	5.62E-13	51.5[b]
C_3H_8	1.09E-12	26.5[b]	7.90E-13	36.6[b]
C_3H_6	2.63E-11	1.1[b]	3.37E-11	0.9[b]
CO	2.39E-13	121.1[b]	1.94E-13	148.8[b]

[a]Assuming Diel Average [OH] = 8.0E + 5 cm^{-3}.
[b]Assuming diel average [OH] = 4.0E + 5 cm^{-3}.

dropped to a factor of 1.2 to 1.6. For CO, which is approximately 5 times less reactive than propane (Table 2), no significant trend is seen between PWB and TP over 0–8 km altitude at latitudes of 25–45°N. Evidence of this can be found in the altitude/latitude grid plots for CO shown in Figure 2a (1 and 2). Here, no clear concentration trend is obvious. It might be argued that the low latitude zones shown in these figures might suggest a trend in CO based on the data at latitudes of 15–20°N for PWB. However, a more detailed inspection of these data has shown that this 2 1/2 km altitude segment reflects an extraordinary sampling encounter with an urban plume. In this case, the aircraft was imbedded in the same pollution plume for over 1 hour. For example, the altitude/concentration plot for the 5–25°N region (i.e., Figure 1c), which excludes this grid segment, reveals only a slight difference between the two studies, TP being slightly higher.

[19] Shifting to precursors which have an even more direct role in controlling O_3 photochemistry (e.g., H_2O, NO), it can be seen from Figure 1d that H_2O levels are typically higher during TP. The difference factor, however, is quite modest, e.g., 1.5 for the 25–45°N sector. For the critical O_3 forming precursor NO (i.e., Figure 1e), the difference between studies is again modest (difference factors typically $\leq$1.6). In this case, at latitudes of 25–45°N TP NO levels are higher, but for 5–25°N the reverse is true (e.g., <8.5 km), i.e., PWB levels are higher. However, the higher levels of NO at 25–45°N do raise the question: is this increase due to higher mainland emissions rates or are other factors involved? The answer we believe does not lie in enhanced emission rates for three reasons: (1) the 5–25°N latitude zone shows the opposite trend; (2) the average difference factor of 1.5 is substantially larger than recent emission inventory data would suggest (e.g., 10–15% over an ~7 year period) [*Streets et al.*, 2003]; and (3) the calendar shift in the sampling windows of TP would tend to favor higher NO levels due to increases in continental deep-convective events [e.g., *Pickering et al.*, 1990, 1993; *Kumar et al.*, 1995; *Levy et al.*, 1996; *Crawford et al.*, 1997a].

4.2. Airborne Ozone Profiles

[20] An interesting aspect of O_3 is that although it can be a final product of photochemistry, it also is a precursor species in that its photolysis initiates new HO_x radical formation. It is this radical production which facilitates the oxidation of CO, CH_4, and NMHCs, leading to more O_3 (i.e., it takes O_3 to make O_3). It is a species, therefore, whose distribution can reflect the intensity of springtime photochemistry as well as that of strat-trop exchange. As shown in Figures 2b(1) and 2b(2)), the PWB and TP data provide a contrasting picture of O_3. For example, at higher latitudes there is a noticeable shift toward higher O_3 values during TP. This trend is quite evident for latitudes >30°N and altitudes <8 km, where the concentration range of O_3 is 30–50 ppbv for PWB but 5–70 ppbv for TP. On the other hand, for latitudes <20°N, the difference between data sets is seen as relatively small. This point is made even more clear in the altitude/[O_3] plots (Figure 1f). For the latitude range of 5–25°N, the typical difference is less than 10 ppbv. Perhaps even more importantly for this latitude range there is no systematic trend evident. By contrast, for the latitude range of 25–45°N, the TP median O_3 value is 15 to 22 ppbv higher than for PWB.

[21] Further confirmation of this trend in the large-scale picture for O_3 in PWB and TP was demonstrated by examining the altitude/latitude O_3 plots constructed from the airborne DIAL (Differential Absorption Lidar) data [*Browell et al.*, 1998, 2003b; *Crawford et al.*, 1997a]. These data represent an independent determination of the concentration levels of tropospheric O_3. They are unique in that continuous spatially resolved vertical profiles of O_3 were recorded during each flight. Thus the DIAL instrument generates a much larger O_3 data base than is possible with the airborne in situ measuring instrument. The results from this analysis are shown here in Figures 3a and 3b. Quite apparent from these is that for latitudes >25°N and altitudes $\leq$8 km, PWB O_3 mixing ratios tend to fall into the 40–60 ppbv range; whereas, for TP there are considerable areas of the plot showing O_3 reaching the 60–75 ppbv range. At the semi-quantitative level therefore reasonable agreement appears between the in situ and DIAL O_3 data bases. (Note that further discussion of the DIAL data appears in section 4.3.)

4.3. Photochemical Model Product Profiles

[22] Based on the PWB and TP observational data, it is evident that there is no single trend that fits all O_3 precursor species. This is particularly true for the latitude range of 25–45°N. For moderately reactive to very reactive NMHCs, the trend is one involving PWB concentration levels exceeding those seen in TP at virtually all altitudes. This is obviously counter to what one might predict from the latest emission inventory data [e.g., *Streets et al.*, 2003]. H_2O and NO levels, on the other hand, were slightly higher during TP. CO, by contrast, revealed almost no systematic difference between the two field studies. Finally, for O_3 itself, the TP data were found to exceed those of PWB by 15 to 22 ppbv at all altitudes for the above cited high latitude zone but not for 5–25°N. Thus it could be concluded that the collective results from the O_3 precursors analysis have not convincingly demonstrated that Pacific Rim trace gas emissions have risen significantly in the 7 years between PWB and TP. (Note that this point is more extensively discussed in section 4.3.)

[23] Given the above trends in O_3 precursor species, the photochemical model products that most relate to O_3 photochemistry can now be examined, e.g., $J(O^1D)$, OH,

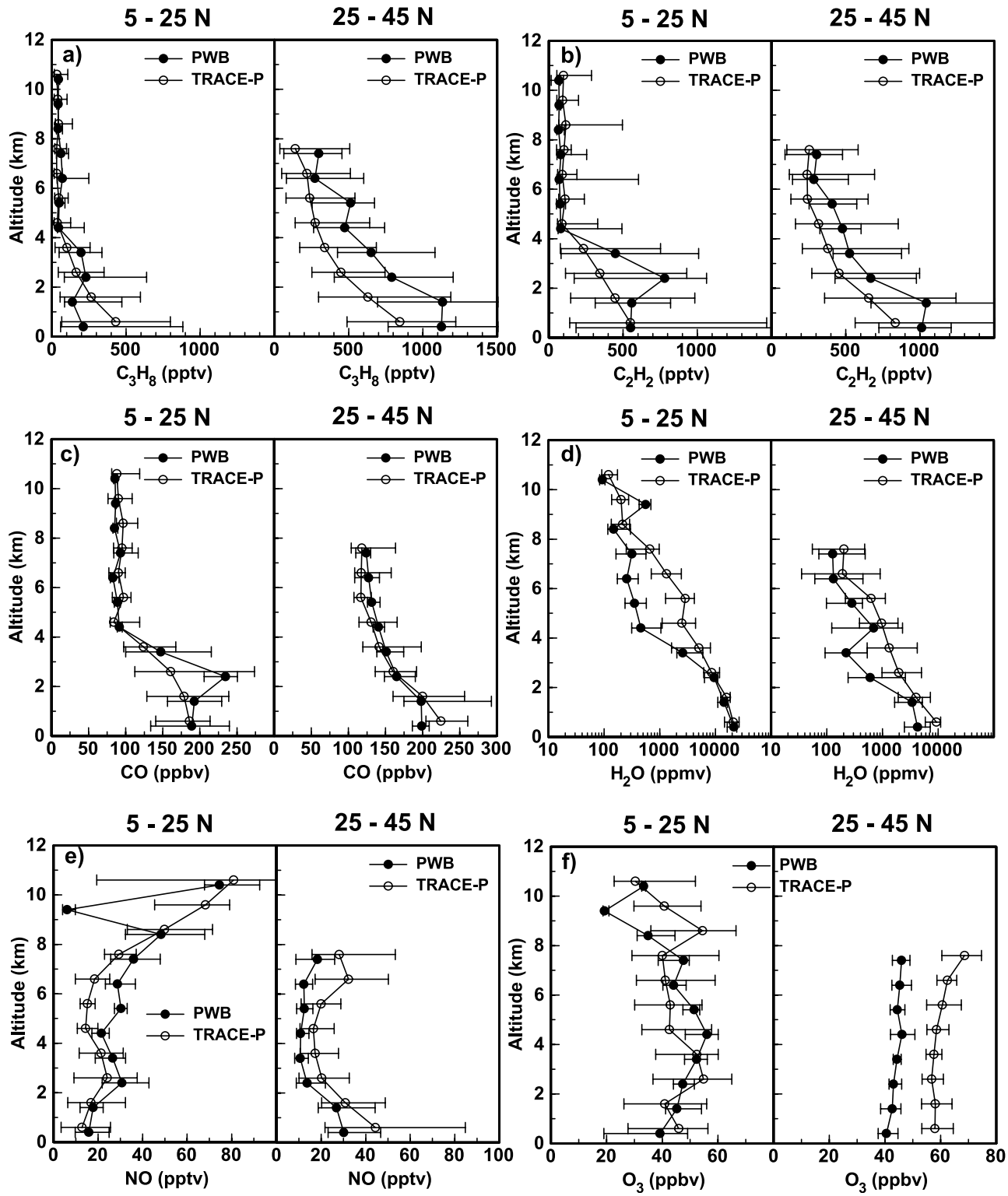

Figure 1. Altitude versus concentration plots for (a) C_3H_8, (b) C_2H_2, (c) CO, (d) H_2O, (e) NO, and (f) O_3. Left panel shows median values and inner quartiles for 5–25°N; right panel shows similar type information but for 25–45°N. Median values shown were estimated by binning all data within one kilometer of altitude across the indicated latitude zone.

HO_2, $F(O_3)$, $D(O_3)$, and $P(O_3)$. The objective here, as in the case of the assessment of O_3 precursors, will first be to simply compare the absolute values for each photochemical parameter as estimated from the PWB and TP data sets. Finding any differences, the question of "cause" will be explored. This will involve both looking at the impact from precursor level differences between the two studies as well as the impact arising from there being what earlier was

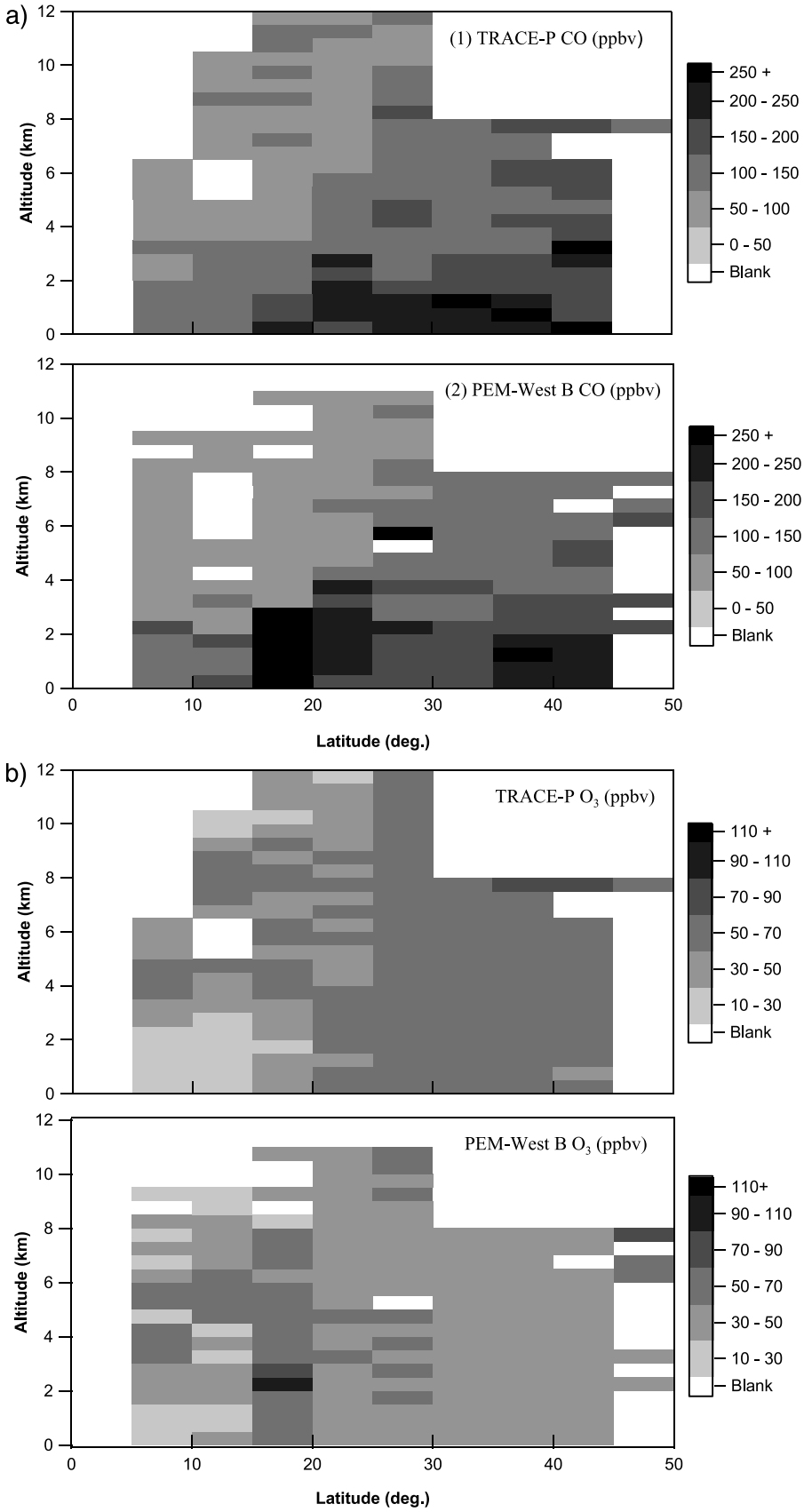

Figure 2. Altitude/latitude grid plots for (a) CO and (b) O_3. Panel 1 shows the observations from TRACE-P; panel 2 shows the observations from PEM-West B. Median values shown were estimated for each grid box, 0.5 km by 5° in size. See color version of this figure at back of this issue.

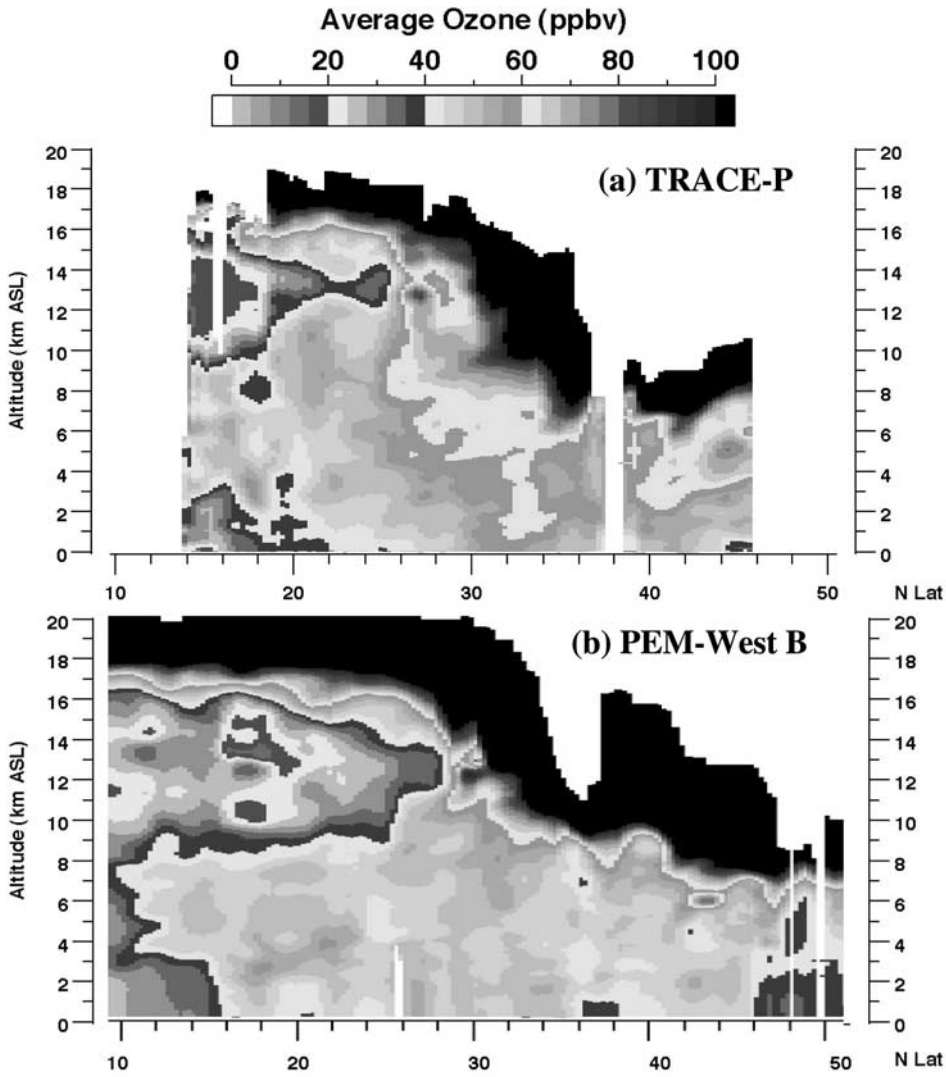

Figure 3. DIAL (Differential Absorption Lidar) O_3 observations as a function of altitude and latitude as observed during TRACE P (a) and PEM-West B (b). See color version of this figure at back of this issue.

described as ''a springtime temporal shift'' in the TP sampling window. To the extent that shifts in the respective sampling windows or differences in the levels of O_3 precursor levels can not explain the differences between programs for the calculated photochemical parameters, other factors will then be explored.

4.3.1. $J(O^1D)$

[24] Shown in Figure 4a are altitude plots of diurnal averaged $J(O^1D)$ for PWB and TP for the latitude zones of 5–25°N and 25–45°N. Recall, the value of $J(O^1D)$ is tightly coupled to the $O(^1D)$ concentration via reaction R1 (e.g., O_3 photolysis); and via reaction R3 which leads to the conversion of $O(^1D)$ into two OH radicals. This reaction sequence defines one of the major primary sources for OH. However, since $J(O^1D)$ is critically dependent on the availability of UV radiation below 315 nm, its value is strongly influenced by shifts in the average daytime solar zenith angle as well as by shifts in the overhead O_3 column density. The combined effects of these controlling factors is quite apparent in Figure 4a in that the average value of $J(O^1D)$ is ~2.5 times larger for the low-latitude zone than for the higher one. That is, at lower latitudes, both a lower average zenith angle and a lower average overhead O_3 column density leads to a higher average UV actinic flux. Quite apparent also from Figure 4a is that the $J(O^1D)$ difference between PWB and TP is much larger for the latitude range of 25–45°N than for 5–25°N. At the higher latitudes, TP values frequently fall into the range of $0.4–0.8 \times 10^{-5}$ s^{-1}; whereas for PWB the typical range is $0.15–0.5 \times 10^{-5}$ s^{-1}, leading to a difference factor between them that quite often exceeds 2. Further to the south (e.g., 5–25°N), although TP $J(O^1D)$ values also dominate, the difference factor drops to ~1.4.

4.3.2. OH, HO_2

[25] The large difference in the value of $J(O^1D)$ between TP and PWB should contribute to higher TP values for OH. Similarly, higher TP OH values should lead to higher values of the closely coupled photochemical species HO_2. Shown

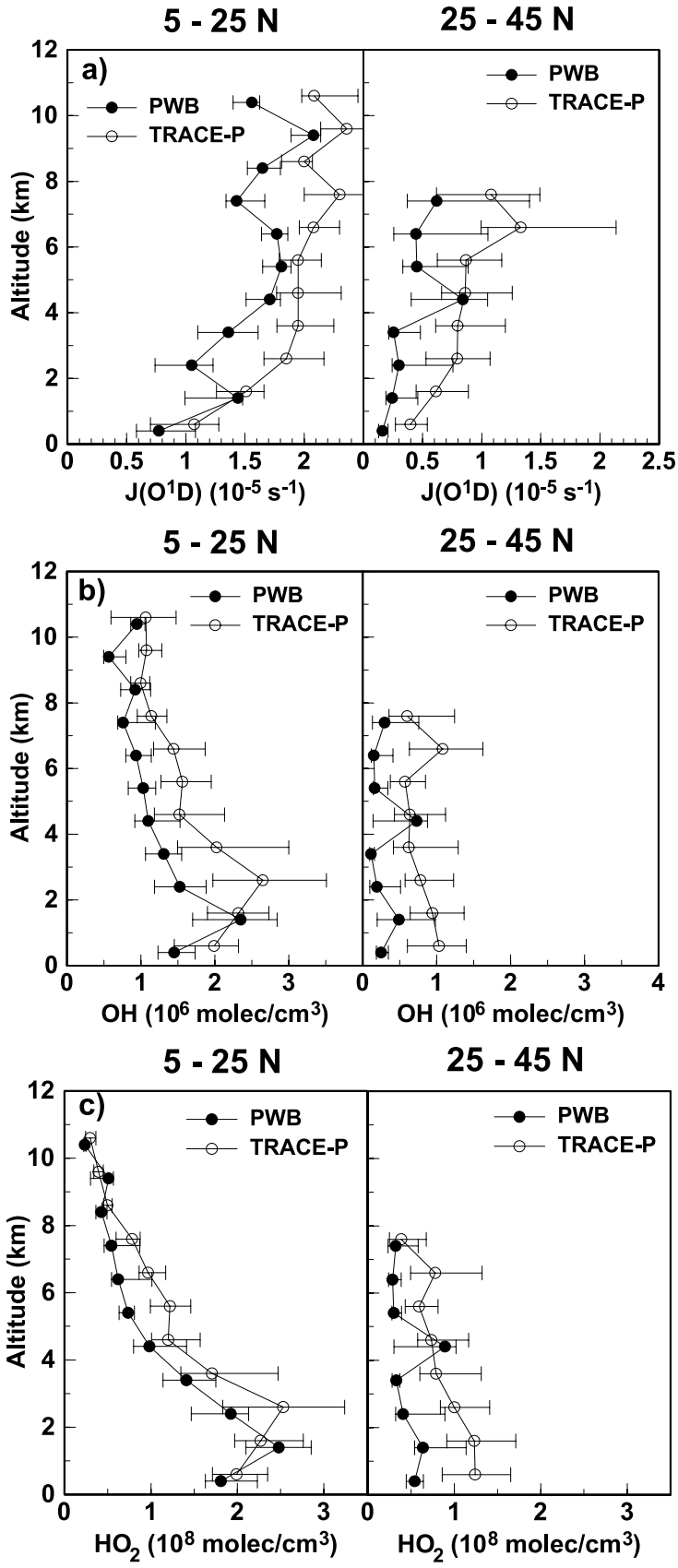

Figure 4. Model predicted vertical distributions for (a) $J(O^1D)$, (b) OH, and (c) HO_2. Left panel shows median values and inner quartiles for 5–25°N; right panel shows similar type information but for 25–45°N. All values are 24-hour averages. Medians were estimated by binning all calculated values within one kilometer of altitude across the indicated latitude.

in Figures 4b and 4c are the altitude/concentration plots for each of these species. For OH, while it is clear that both latitude ranges show TP having higher levels, the difference factor between the two programs is substantially larger for the high-latitude zone. As suggested above, the difference at these latitudes is similar to that for $J(O^1D)$, e.g., frequently greater than a factor of 2. However, the fact that the trend in OH tracks the trend in $J(O^1D)$ reflects both the major role played by $J(O^1D)$, as well as the supporting role defined by slightly higher precursor concentration levels for H_2O, NO, and O_3 found during TP. Not surprisingly, as seen in Figure 4c, a similar trend exists for HO_2. At the higher latitudes, this resulted in TP values being over a factor of 2 greater than for PWB. (Note that TP observational values for HO_2 as well as those for other radical species and their comparison with model predictions can be found in the work of *Cantrell et al.* [2003].)

4.3.3. $F(O_3)$, $D(O_3)$, and $P(O_3)$

[26] Having demonstrated that photochemical activity was significantly elevated during TP relative to PWB, as defined in terms of the values of $J(O^1D)$, OH, and HO_2, it follows that this heightened level of photochemistry should be reflected in the values for photochemical O_3 formation, $F(O_3)$, destruction, $D(O_3)$, and tendency, $P(O_3)$. However, for the latter parameter, establishing the trend is not as straight forward. Unlike $F(O_3)$ and $D(O_3)$, $P(O_3)$ represents the difference between two numbers that are typically similar in magnitude (i.e., equation (3)); and since both $F(O_3)$ and $D(O_3)$ tend to increase with an increase in photochemical activity, the difference between these two terms can easily change sign. Thus the final outcome is often dictated by the level of NO. More specifically, it depends on how much larger the observed NO is than the "critical" NO, NO_{crit}. (NO_{crit} is defined as that NO concentration required to make the numerical value of equation (3) approximately equal to zero, i.e., the rate of photochemical O_3 formation is exactly balanced by the rate of photochemical destruction.)

[27] Shown in Figures 5a and 5b are the values of $F(O_3)$, and $D(O_3)$ plotted in the same format as used earlier. The 25–45°N latitude zone, in particular, shows a pronounced effect due to enhanced TP photochemistry. Here values of $F(O_3)$ typically exceed those for PWB by factors of 2 to 4. (Recall that both NO and HO_2 (Figures 1e and 4c) were also substantially higher for TP for this latitude zone.) By contrast, for 5–25°N (Figure 5a) the difference between TP and PWB is seen as being quite modest. This most likely reflects the fact that the two most critical species controlling the values of $F(O_3)$, HO_2 and NO, have opposite trends at these low latitudes. For both latitudinal zones, however, >65% of the $F(O_3)$ value can be attributed to reaction R4 (i.e., HO_2), while the NMHC channel, R6, typically contributed <15%. This means that the earlier cited NMHC differences between PWB and TP have had little or no impact on the current assessment of O_3 photochemistry in the northwestern North Pacific.

[28] In Figure 5b, values of $D(O_3)$ are shown as a function of altitude. Once again, as in the case of $F(O_3)$, the largest difference between the two airborne studies is that at high latitudes. Here, TP values are typically factors of 2–6 greater than those for PWB. By contrast, at low latitudes the difference between studies is typically closer to a factor of 1.5, TP being higher. The higher values seen for TP can be understood in terms of the higher values of $J(O^1D)$ as well as higher levels of water (e.g., Figure 1d). Reflecting this, greater than 60% of all O_3 destruction could be assigned to the reaction sequence R1 and R3 (i.e., $O(^1D)$). In contrast, at 25–45°N all three O_3 destruction processes (i.e., R3, R7, and R8) were found to make substantial contributions.

[29] Estimates of the net photochemical effect on O_3 (equation (3)) are summarized in Table 3. For the high-latitude zone (25–45°N), $P(O_3)$ values are seen as being generally more positive for TP than for PWB. This is particularly true at very low altitudes (0–1 km) where the TP value is nearly a factor of 2 larger than that for PWB. However, over the most significant altitude range (i.e., that having the biggest influence on O_3 trends, 1–8 km), the difference between the two studies drops to ~1.4, TP again being higher. Perhaps, more importantly, is the observation that for both studies $P(O_3)$ values are positive (e.g., average column values of 0.5 and 0.7 ppbv/day) over the altitude range of 1–8 km. This finding indicates that not only is O_3 building up during early spring due to photochemistry but that the rate of the build-up accelerates as the spring season continues to develop. It should be noted, however, that such behavior is not limited to only the northwestern North Pacific. Similar levels of build-up have been reported from the data collected during the TOPSE airborne field program, a study that focused on Northern Canada and Greenland [e.g., see *Browell et al.*, 2003a; *Wang et al.*, 2003, and references therein].

[30] As suggested earlier in the text, one of the major reasons why both PWB and TP show positive values for $P(O_3)$ at high latitudes is that NO_{obs} exceeds NO_{crit}. The importance of this point is amplified on here in the form of Figure 6 which shows the altitudinal trends in both NO_{obs} and NO_{crit} for the high-latitude zone, 25–45°N. Quite apparent is that both field studies have NO_{obs} levels well in excess over that required to produce net O_3 (i.e., $NO_{obs} > NO_{crit}$). However, it is also evident that of the two studies TP tends to show, on average, a larger difference between NO_{obs} and NO_{crit}. This larger difference contributes to higher values of P(O3) for TP.

[31] At low latitudes, things are quite a bit different as shown in Table 3. Large $D(O_3)$ and $F(O_3)$ values (e.g., upwards of 7 ppbv/day) lead to significantly different results for the two studies. PWB shows slightly positive values at most altitudes, whereas those for TP are negative. Thus for an altitude range of 1–11 km PWB is seen generating an overall column average value of +0.63 ppbv/day, whereas TP is seen as only achieving a neutral situation, having an

Figure 5. (opposite) Model predicted vertical distributions for (a) $F(O_3)$ and (b) $D(O_3)$. Left panel shows median values and inner quartiles for 5–25°N; right panel shows similar type information but for 25–45°N. Medians were estimated by binning all calculated values within one kilometer of altitude across the indicated latitude.

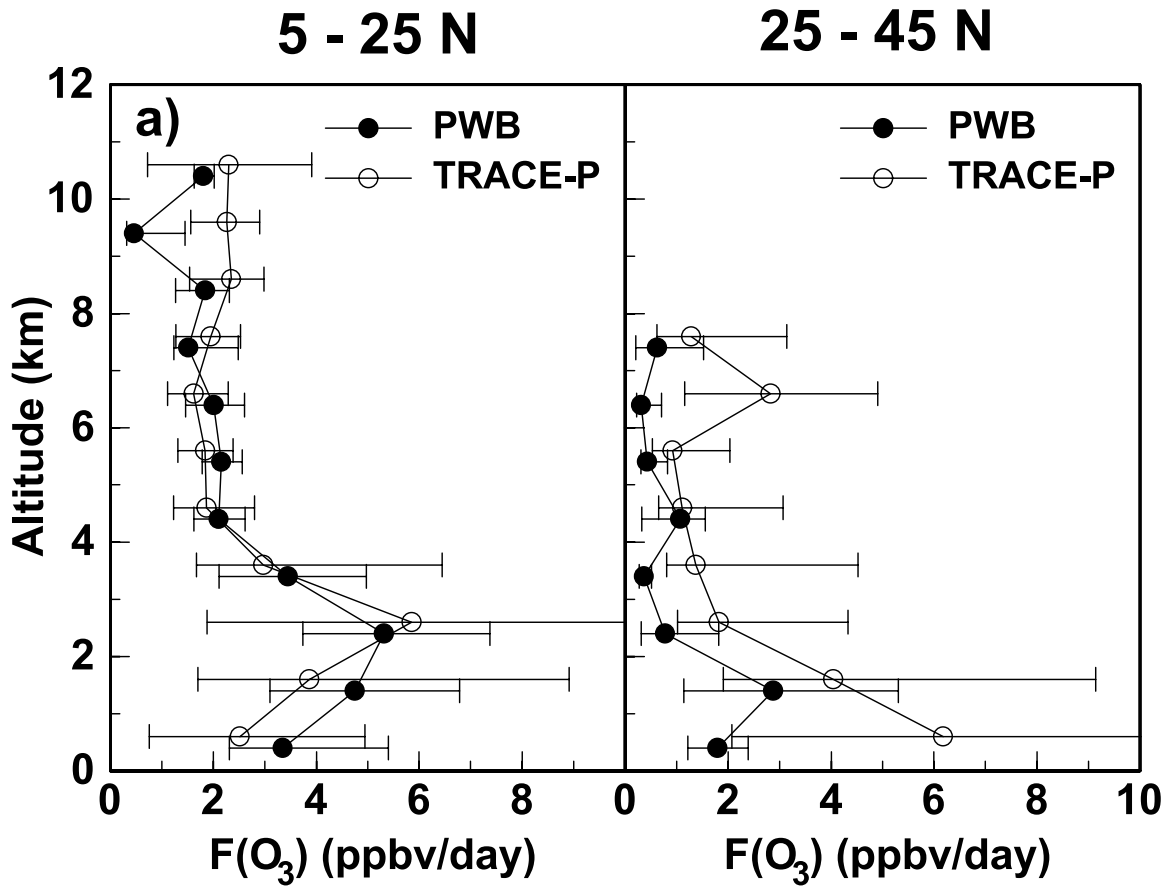
5 - 25 N
25 - 45 N
a)
PWB
TRACE-P
Altitude (km)
F(O3) (ppbv/day)
F(O3) (ppbv/day)

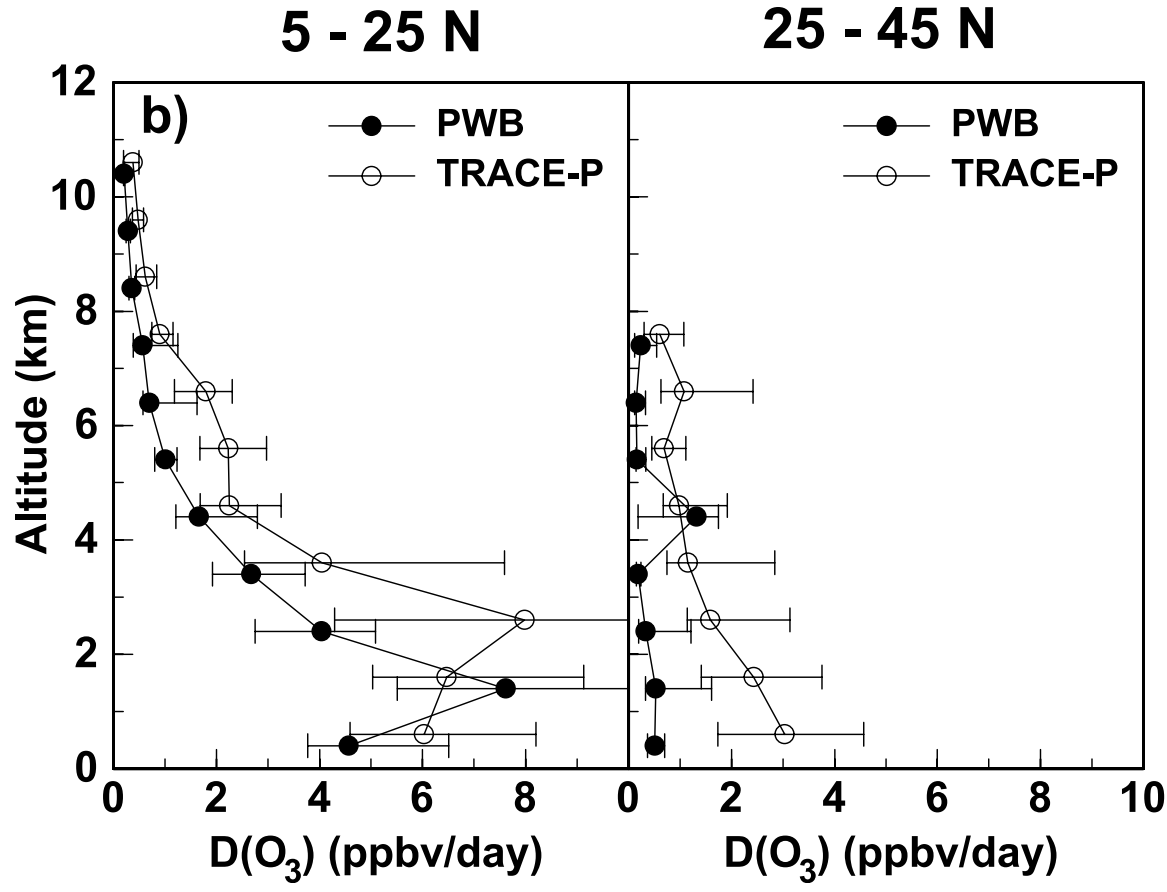
5 - 25 N
25 - 45 N
b)
PWB
TRACE-P
Altitude (km)
D(O3) (ppbv/day)
D(O3) (ppbv/day)

Table 3. Comparison of P(O3) Value Between PEM-West B and TRACE-P

Latitude Range, deg. N	Altitude Range, km	PWB $P(O_3)$ Avg.[a], ppbv/day	TP $P(O_3)$ Avg.[a], ppbv/day
5–25	0–1	−1.22	−3.51
	1–4	−0.27	−1.93
	4–8	0.97	0.03
	8–11	1.09	1.82
	1–8	0.44	−0.81
	1–11	0.63	−0.02
25–45	0–1	1.28	3.14
	1–4	0.99	0.69
	4–8	0.14	0.69
	1–8	0.50	0.69

[a]Averages computed from data shown on Figures 5a and 5b; $P(O_3) = F(O_3) - D(O_3)$.

average column value of −0.02 ppbv/day. In this case it is found that for TP, NO_{crit} tends to exceed NO_{obs} at most altitudes, whereas for PWB NO_{crit} typically is smaller than NO_{obs}.

4.4. Detailed Photochemical Assessment and Corroborative Ozonesonde Data

[32] As discussed in section 4.2, the precursor data from TP and PWB give mixed trends, some species being higher during TP, others being more elevated in PWB. Quite apparent also was the finding that the latitude zone experiencing the largest number of differences between the two studies is that defined here as 25–45°N. While some of these differences may indeed have been influenced by modest shifts in anthropogenic or bioemission rates for a given precursor species over the last 7 years, the evidence presented here indicates that most of them can best be understood in terms of the enhanced photochemical activity encountered during TP. For example, in the case of C_3H_8 and C_3H_6 the trend is opposite to what might be predicted based on updated emission inventory data [*Streets et al.*, 2003]. The chronologically earlier PWB study is seen as having higher values than TP. However, from an examination of Table 2, it is quite evident that the systematic shift in the average OH value from 6 March to 25 March results in a substantial reduction in the estimated lifetimes for OH reactive species like propane or propene (i.e., a factor of 2). This trend, however, would be expected only for species having relative short lifetimes, i.e., shorter than the seasonal separation time for the two studies of ~3 weeks and for which the transport times from source region to sampling location were similar. For CO, which is indicated to have a lifetime of approximately 2 months (compared with 13 days for C_3H_8), the influence from OH chemistry would neces-

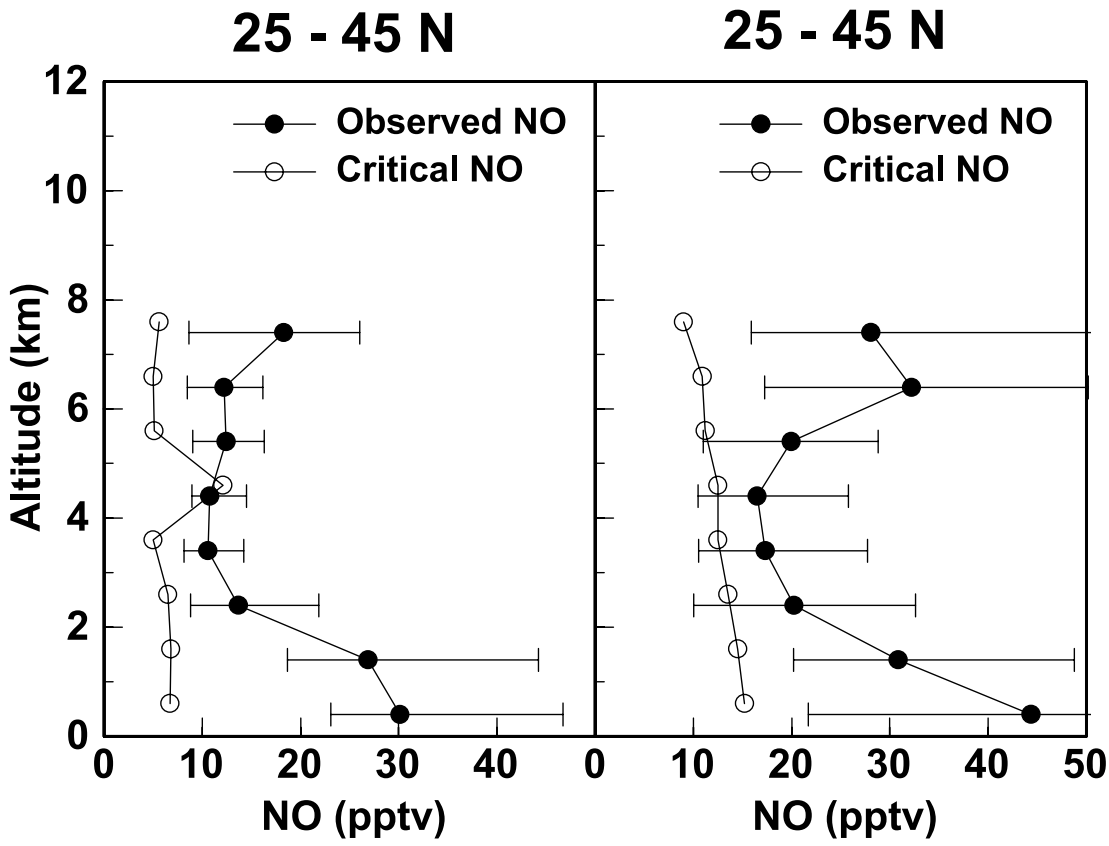

Figure 6. Altitudinal comparisons of NO observations (median and inner quartile values) with model estimated critical NO values at 25–45°N for PEM-West B (left panel), TRACE-P (right panel). Median values were estimated by binning all data or calculated parameter within one kilometer of altitude across the indicated latitude zone.

sarily be greatly dampened. As shown earlier in Figure 1c, this indeed is what is seen in the two vertical profiles for CO in that they are quite similar.

[33] Having found evidence indicating that the 3-week shift in the sampling window of TP might account for many of the differences between the two studies, as related to OH sensitive O_3 precursor species, the question remains what is responsible for the enhancement in photochemistry? As previously noted, this could involve either shifts in solar conditions, changes in chemical conditions over this brief period or some combination of both. That shifts in solar conditions represent the major reason can be found in our earlier analysis of $J(O^1D)$ values which revealed that TP values were typically two or more times larger than those for PWB at high latitudes. Further analysis of these $J(O^1D)$ values has also shown that nearly half of the TP $J(O^1D)$ change (relative to PWB) is due to decreases in the solar zenith angle, the remainder being largely due to decreases in the overhead O_3 column density. The latter change, however, is somewhat more complicated than this in that a significant fraction of the overhead O_3 column shift may have been a result of a sampling bias toward higher latitudes during PWB.

[34] Additional sensitivity tests related to the impact from chemical changes, have suggested that the cited differences between each program's NO and H_2O levels were not as important to the photochemical enhancement as was the shift in $J(O^1D)$. Given this, with the tight coupling between $J(O^1D)$,OH and HO_2, it follows that the major factor driving the difference in O_3 levels between the two campaigns was primarily the shift in the UV actinic flux. A much smaller effect resulted from the higher concentration of NO in TP, specifically the larger difference between NO_{obs} and NO_{crit}.

[35] Finding that both PWB and TP showed significant positive values for $P(O_3)$ (e.g., 1–8 km average, 0.5 and 0.7 ppbv/day, respectively) strongly suggests that O_3 levels were most likely on the increase due to photochemistry throughout the time period of both campaigns. Given this, along with the assumption that this build-up was not limited to just the Pacific Rim region but was occurring at a similar rate on a global scale at these same latitudes (e.g., see earlier reference to TOPSE findings) [*Wang et al.*, 2003], an upper limit value for the increase in O_3 can be estimated reflecting the 3-week separation period. For this estimate, the "average" $P(O_3)$ value for TP of 0.7 ppbv/day (1–8 km) for 20 days (separation time) was used, leading to a ΔO_3 increase of 14 ppbv. This value is seen as being slightly lower than the cited airborne range of 15–22 ppbv but is clearly within the uncertainties of the calculations and observations.

[36] Using the independently recorded NASA UV DIAL O_3 data (e.g., Figure 3), a more quantitative assessment of these DIAL data has produced a median ΔO_3 value of 9 ppbv with an inner quartile range of 5 to 11 ppbv. Thus in this case the model estimated value of ΔO_3 quite easily can explain the DIAL estimated ΔO_3 value for the two studies. These results then add to the strength of our earlier argument that most of the differences between the two field studies, including the ΔO_3 value, can be explained in terms of the 3-week shift in the spring sampling window of TP relative to PWB.

[37] That we have chosen in the above calculations to look at the photochemical production of O_3 on a global scale rather than regionally is a reflection of two factors. First, during early spring the lifetime for O_3 is still relatively long, and second, that the major sources of NO_x, CO, and NMHC's exist at many different global locations. It is quite likely, therefore, that there would be an integrated build-up of O_3 due to its photochemical production on a global scale. In this context, the impact from a circulating band of pollution that could be periodically energized by NO_x generated from lightning or other high altitude NO_x sources has been previously addressed by *Davis et al.* [1996], *Liu et al.* [1996], *Crawford et al.* [1997a], and more recently by *Liu et al.* [2002]. Liu et al., in particular, examined the ozonesonde data in East Asia and concluded from their analysis that it is during the springtime period that Asian emissions make their biggest impact on exported O_3.

[38] In an effort to corroborate the above photochemical conclusion, presented here are 10 years of Japanese ozonesonde data. Since these stations all lie well within the PWB/TP study region, it can be argued that they should give some reading on whether or not there has been a long-term upward trend in O_3 for this region. In addition, they should provide an excellent basis for evaluating the seasonal trends in O_3. The stations involved in this exercise were those at Naha, Kagoshima, Tsukuba, and Sapporo. They span the latitude range of 26 to 43°N. All four stations used similar instrumentation and a common data sampling protocol (available at www.msc-mc.ec.gc.ca/woudc/data/index_e.html). As seen in Figures 7a and 7b, the 10-year summary data from the representative stations of Kagoshima, 31.6°N, and Sapporo, 43.1°N indicate that for the month of March there is very little change in O_3 levels over the time span of 1991 to 2001. In fact, there are more cases at the three altitudes examined when the slope is slightly negative than positive. In Table 4 a more quantitative analysis of the data shown in Figures 7a and 7b is presented along with those from the other two Japanese stations, Naha and Tsukuba. For the month of March, all four stations show 10-year trends that typically lead to shifts of less than 1.2 ppbv/yr with more than half of the slopes shown being negative. Thus these results would appear to support those drawn above, based on the airborne data, namely, that once the effects of the 3-week shift in the TP sampling window are taken into consideration, there is little or no evidence of a significant long term trend in O_3.

[39] To gain further insight about the seasonal information imbedded in the ozonesonde data, the average monthly values were plotted for the time period of January–April as shown in Figures 8a and 8b. As in the earlier plots, the data base was that recorded from 1991 to 2001 at Kagoshima and Sapporo. As seen from the plots, the results are quite convincing in that the data clearly show a positive trend in O_3 at all three altitudes over the time period specified. From these plots, it can be estimated that from early March to late March the absolute increase in O_3 ranges from 5–7 ppbv. Other investigators have examined still other Japanese ozonesonde data sets, but for the earlier years of 1980–1995 [*Logan et al.*, 1999]. These have produced similar seasonal trends over the spring time period. Thus the Japanese ozonesonde data qualitatively appear to also support our airborne-based conclusions about the impact from a 3-week shift in sampling during springtime. They do not agree, however, when examined on a more quantitative

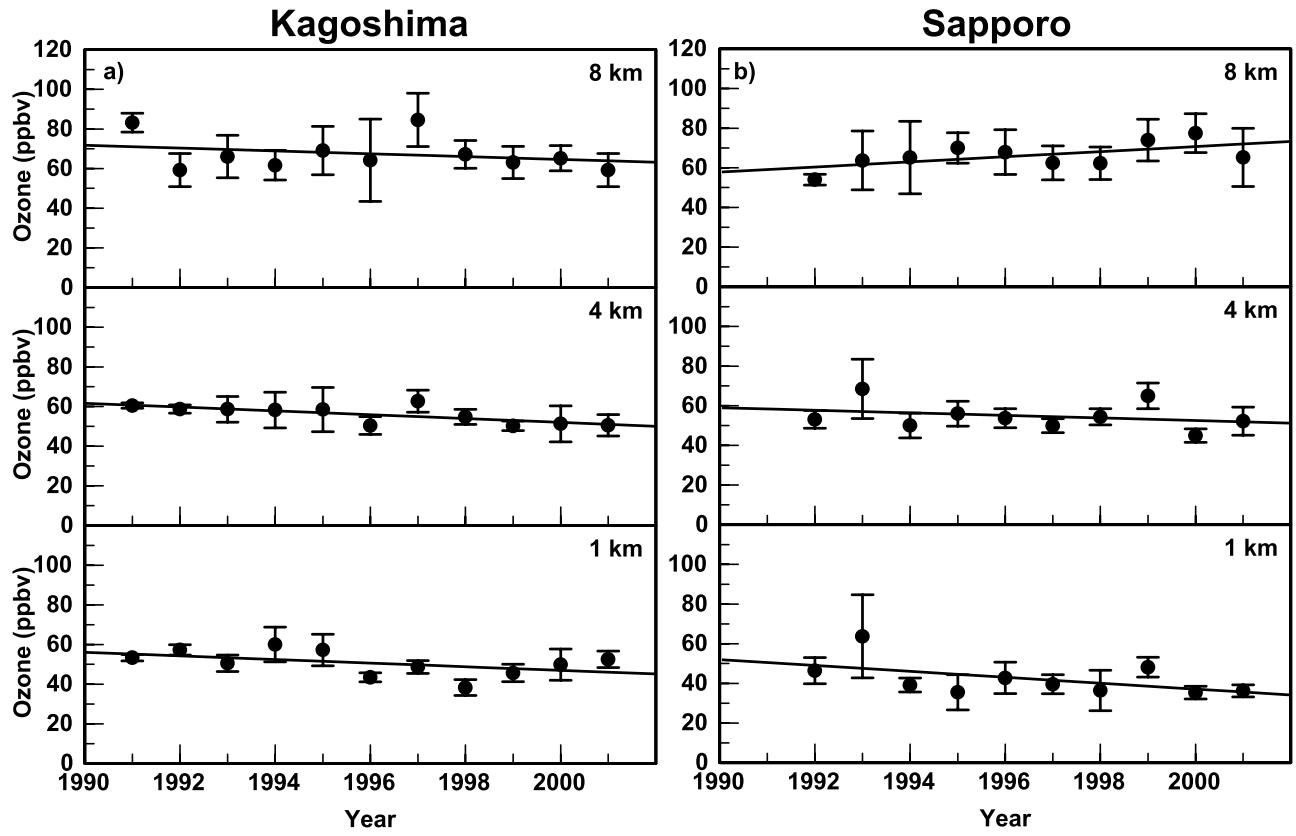

Figure 7. Long-term ozone trends as defined by ozonesonde data from (a) Kagoshima and (b) Sapporo, Japan. Data points represent averages estimated over a 1 month period for each year for the three altitudes 1, 4, and 8 km. Values for each central altitude were estimated from data recorded ±0.5 km of the central altitude. Error bars represent one standard deviation.

level. The absolute magnitude of the ozonesonde ΔO_3 increase is somewhat more than a factor of 2 lower than the model estimates of ΔO_3 and factors of 1.5 and 3 lower when compared to the DIAL and in situ values.

[40] Possible reasons for this disagreement include the variability in the year to year ozonesonde observations, the degree of overlap between the aircraft and ozonesonde data collection sites and the possibility of systematic errors in one or more of the cited measurement systems. As can be seen from the ozonesonde statistics reported in Table 4, one standard deviation at any of the three altitudes for the month of March typically can range from 4 to 8 ppbv. And although both the ozonesonde and aircraft observations fell within the larger sampling domain defined here as the northwestern North Pacific/Pacific Rim, the specific sampling sites covered by each within this domain differed considerably. In this context any inhomogeneities within the domain could have resulted in somewhat different data bases being recorded, thus influencing the representativeness of the respective studies. (As assessed by *Wild et al.* [2003], this is more likely to have occurred during PWB due to the more limited number of sampling flights involved.) It

Table 4. Summary of Longer Ozone Trend and Monthly Averages as Derived From Japanese Ozonesonde Data

		1 km		4 km		8 km	
Altitude		Slope, ppbv/year	Mon. Avg., ppbv	Slope, ppbv/year	Mon. Avg., ppbv	Slope, ppbv/year	Mon. Avg., ppbv
Naha 26.2°N	Feb.	−1.3 ± 0.5	45 ± 6	−0.8 ± 0.4	51 ± 5	−1.3 ± 1.2	55 ± 13
	Mar.	0.4 ± 0.4	44 ± 4	0.6 ± 0.7	55 ± 7	−0.7 ± 0.6	59 ± 6
	Apr.	0.5 ± 0.5	44 ± 5	−0.7 ± 0.7	59 ± 7	−0.9 ± 0.6	69 ± 7
Kagoshima 31.6°N	Feb.	−0.6 ± 0.5	42 ± 5	−0.2 ± 0.6	49 ± 6	0.7 ± 0.9	60 ± 9
	Mar.	−0.9 ± 0.6	51 ± 6	−1.0 ± 0.3	56 ± 5	−0.7 ± 0.8	68 ± 9
	Apr.	−1.1 ± 0.6	53 ± 7	−0.5 ± 0.5	60 ± 6	−1.0 ± 0.7	71 ± 8
Tsukuba 36.1°N	Feb.	−0.3 ± 0.3	40 ± 3	−0.1 ± 0.3	48 ± 3	−0.2 ± 0.5	61 ± 5
	Mar.	−0.9 ± 0.3	48 ± 4	−0.3 ± 0.2	53 ± 3	0.8 ± 0.4	62 ± 4
	Apr.	−0.6 ± 0.8	62 ± 8	−0.2 ± 0.4	61 ± 4	0.1 ± 0.6	69 ± 6
Sapporo 43.1°N	Feb.	0.1 ± 0.3	34 ± 3	0.8 ± 0.4	48 ± 5	−0.1 ± 0.6	62 ± 6
	Mar.	−1.5 ± 0.8	42 ± 9	−0.6 ± 0.7	55 ± 7	1.3 ± 0.5	66 ± 7
	Apr.	−0.4 ± 0.7	47 ± 7	0.3 ± 0.4	60 ± 4	−0.7 ± 1.0	71 ± 10

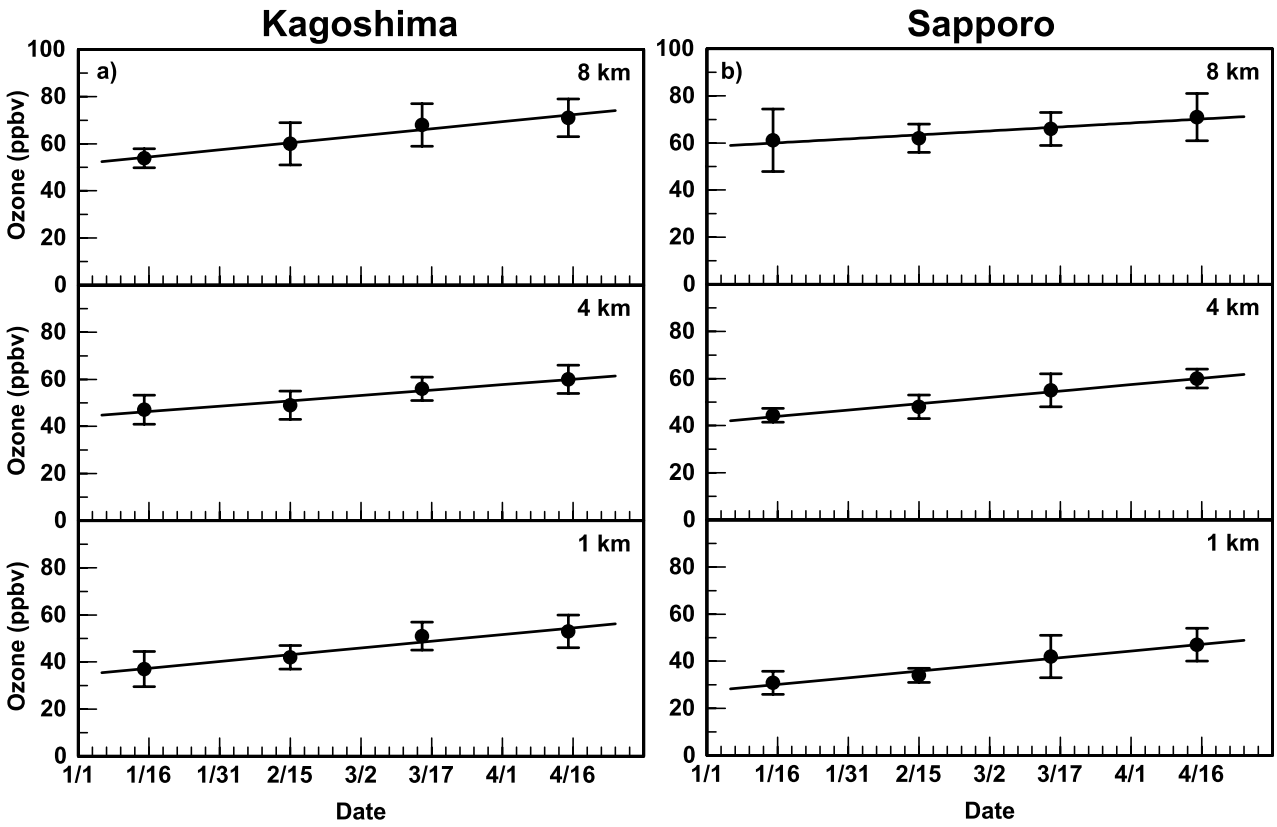

Figure 8. Averaged seasonal ozone trend as defined by ozonesonde data from (a) Kagoshima and (b) Sapporo, Japan. Data points represent average values estimated for each month for the time period of 1991 to 2001 at 1, 4, and 8 km. Values for each central altitude were estimated from data recorded ±0.5 km of the central altitude. Error bars represent one standard deviation.

also must be recognized that not only did the two aircraft studies have different sampling scenarios within this domain but that both of these studies were even more different than the sampling defined by the land-based ozonesonde data collection network. Finally, one must consider the possibility of unknown systematic errors either in the ozonesonde observations or in the aircraft detection systems (i.e., in situ or DIAL) as a basis for disagreement between different studies. Recall that earlier in the text a comparison of the aircraft in situ O_3 results against the independently recorded UV DIAL data produced estimates of ΔO_3 that differed by a factor of 2. This occurred even though both instruments were on the same sampling platform; however, as noted earlier, the DIAL system did sample a much larger cross section than was possible with the in situ instrument.

[41] In spite of the above list of potential problem areas, it seems highly probable that these collective data do point to the high likelihood that the 3-week extension of the TP sampling window into later spring did result in higher observed O_3 levels being seen during the TP field study. It is estimated here that this produced at least a 6 ppbv ΔO_3 difference between studies, but this value could quite possibly be as high as 15 ppbv.

4.5. Stratospheric Versus Photochemical O_3

[42] Given the high probability that a shift in the sampling window of TP relative to PWB led to most of the photochemically induced increase in O_3, the question remains whether other factors might have contributed to the observed O_3 enhancement. The most obvious of these is transport from the stratosphere. During late winter and earlier spring, it is well established that at midlatitudes significant strat-trop exchange can occur [e.g., *Danielsen*, 1968; *Gidel and Shapiro*, 1980; *Mahlman et al.*, 1980]. The relative importance of this source has been evaluated here by contrasting the magnitude of this source against that assigned to photochemistry. The latitude range of comparison is that for which the largest shift in O_3 was observed, 25–45°N. In this evaluation the stratospheric source has been derived from the literature, whereas the photochemical quantity has been estimated from the current model simulations.

[43] Concerning strat-trop exchange, there have been several previous efforts made to evaluate this [e.g., *Gidel and Shapiro*, 1980; *Mahlman et al.*, 1980]. Most of these earlier efforts, however, have been limited to values estimated for the entire Northern or Southern Hemisphere. More recent modeling efforts have attempted to refine these earlier estimates and have, among other things, provided some seasonal and latitudinal definition to this modeling product [e.g., *Lelieveld and Dentener*, 2000; *Appenzeller et al.*, 1996]. In this context, the stat-trop O_3 source for the northern hemisphere during springtime has been evaluated for latitudes of 20–60° by *Wang et al.* [1998] based on *Appenzeller* [1996] with a final result of 8.7×10^{10} molec/cm^2/s. However, other evidence suggests that

strat-trop exchange may have been more intense during TP versus that during PWB. The DIAL observations for the two campaigns, as shown earlier in Figures 3a and 3b, as well as the more detailed analysis of these collective data sets by *Browell et al.* [2003b] point toward this modified viewpoint. For example, from the above-cited figures, it can be seen that over the latitude range of 25–45°N TP O_3 concentrations tend to show 30–40% higher levels in the upper troposphere than for PWB. It can also be seen that major O_3 gradients extend from the tropopause downward into the upper and middle troposphere.

[44] Having assessed the O_3 column flux for strat-trop exchange, it is now possible to compare this quantity with that based on photochemistry. In this comparison, however, it is essential that one compare source against source (e.g., strat-trop exchange versus $F(O_3)$ not $P(O_3)$) since $D(O_3)$ does not distinguish between O_3 from the stratosphere versus that made photochemically. As presented above, the two photochemical formation quantities are 2.8×10^{11} and 6.5×10^{11} molec/cm^2/s for PWB and TP, respectively. Given these values, it can be seen that the column-integrated photochemical O_3 flux is 3 to 6 times larger than that from the stratosphere for the TP/PWB study region. Quite independently, *Pierce et al.* [2003] carried out a model analysis of this region for the specific time period of the TP field program and arrived at a somewhat similar conclusion in that they report a value for $F(O_3)$ that is nearly a factor of 7 times larger than the O_3 flux resulting from strat-trop exchange. Both results suggest then that for the latitude region of interest a substantial influx of stratospheric O_3 took place but that this flux was considerably smaller than that generated from photochemistry. Thus if indeed the strat-trop O_3 flux was somewhat more intense during TP this would help explain a small component of the ΔO_3 difference between the two field studies. However, as already noted, the strat-trop flux is not the major driver behind this difference.

5. Summary and Conclusions

[45] The current study has carried out a comparison of two major NASA field programs (PWB and TP) both of which were executed under springtime conditions. Although both took place in the spring, they were separated in calendar time by approximately 7 years, PWB being launched first in 1994. Of major concern in this study has been assessing whether any evidence could be found that during this seven year period there were significant shifts in the emission rates of O_3 precursors from Pacific Rim countries in East Asia, and as a result, significant shifts in the level of photochemical activity in the western North Pacific. The most recent trace-gas emission inventory data for East Asia [*Streets et al.*, 2003] indicate that this did not happen. These data suggest that the predictions of the mid-1990s, indicating 5% increases in emissions each year, are not in accord with what actually happened over the last 7 years. The newer inventories reflect the onset of a major economic slow down in much of East Asia, China being a possible exception. Thus emissions of species like NO_x, NMHC's and SO_2 are suggested to have increased by no more than 10–15% over the 7-year separation period between PWB and TP. The current study has assessed the above issue by examining the PWB and TP observations. It has done so by looking at the trends in several photochemical O_3 precursor species, O_3 itself, and several photochemical diagnostic parameters indicative of photochemical activity.

[46] Our findings are consistent with recent emission inventory data in that the western North Pacific Ocean, the primary focus of PWB and TP, showed no major increases in any of the O_3 precursor species that could specifically be attributed to a positive shift in primary emissions. In fact, for short-lived NMHC's, the reverse trend was found, i.e., PWB concentrations were systematically higher than those in TP. However, the behavior of these short-lived NMHCs was found to be consistent with the enhancements in photochemical activity during TP relative to PWB. This was particularly true for the latitude range of 25–45°N. Notable enhancements were found in O_3, OH and HO_2 levels as well as in the O_3 related parameters $J(O^1D)$, $F(O_3)$, $D(O_3)$, and $P(O_3)$. However, when these increases were examined from the perspective of the 3-week shift in the sampling window for TP relative to PWB, nearly all of these enhancements were found to be explicable in terms of increases in photochemical activity. Of central importance to this increase was the UV actinic flux which was found to be over a factor of 2 times larger during TP than PWB (i.e., 25–45°N). This enhancement resulted from systematic decreases in the solar zenith angle and in the overhead O_3 column density. The higher level of photochemical activity during TP also appears to explain much of the observed high-latitude difference found in O_3 between the two field studies. This conclusion reflects model calculations showing a net O_3 production rate of 0.7 ppbv/day (estimated for TP). The latter value was assumed to apply to the latitudinal band of 25–45°N on a global scale for a 3-week time period. The resulting ΔO_3 value of 14 ppbv calculated from the TP and PWB data bases is somewhat higher than that estimated from the airborne DIAL data and from the four Japanese ozonesonde stations, but is lower than that estimated from the aircraft in situ O_3 data. The fact that the variability associated with each of the above estimates does not lead to an effective overlap of values suggests that there may be a modest systematic error in one or more of the estimates. However, it is even more likely that differences in the specific sampling scenarios used to define each of the independent data bases may account for the lack of overlap between them.

[47] Although photochemical production of O_3 is indicated to be the primary reason for the ΔO_3 shift between the PWB and TP studies, some attention was also given to examining the potential role of strat-trop exchange as a source of high latitude O_3 relative to that produced from photochemistry. The results from this comparison showed that during the early spring the photochemical source is 3 to 6 times larger than that from strat-trop exchange. Even so, it is important to recognize that stratospheric air transported into the troposphere not only defines a direct primary source of O_3, it also can serve as photochemical "seed" O_3. This "seed" O_3, in the presence of cotransported NO_x, potentially can lead to further photochemical production of O_3, thereby amplifying the impact from this primary source.

[48] **Acknowledgments.** The author D. Davis would like to acknowledge the partial support of this research from NASA grant NCC-1-01024. He would also like to acknowledge the support given to this project by NASA's aircraft support facility, both at Wallops Island, Virginia, and at Dryden, California.

References

Appenzeller, C., J. R. Holton, and K. H. Rosenlof, Seasonal variation of mass transport across the tropopause, *J. Geophys. Res.*, *101*, 15,071–15,078, 1996.

Atkinson, R., D. L. Baulch, R. A. Cox, R. F. Hampson Jr., J. A. Kerr, and J. Troe, Evaluated kinetic and photochemical data for atmospheric chemistry, Supplement IV, IUPAC subcommittee on gas kinetic data evaluation for atmospheric chemistry, *J. Phys. Chem. Ref. Data*, *21*, 1125–1568, 1992.

Berresheim, H., P. Wine, and D. D. Davis, Sulfur in the atmosphere, in *Composition, Chemistry, and Climate of the Atmosphere*, edited by H. B. Singh, pp. 251–307, Van Nostrand Reinhold, New York, 1995.

Browell, E. V., S. Ismail, and W. B. Grant, Differential absorption lidar (DIAL) measurements from air and space, *Appl. Phys. B*, *67*, 399–410, 1998.

Browell, E. V., et al., Ozone, aerosol, potential vorticity, and trace gas trends observed at high latitudes over North America from February to May 2000, *J. Geophys. Res.*, *108*(D4), 8369, doi:10.1029/2001JD001390, 2003a.

Browell, E. V., et al., Large-scale ozone and aerosol distributions, air mass characteristics, and ozone fluxes over the western Pacific Ocean in late winter/early spring, *J. Geophys. Res.*, *108*(D20), 8805, doi:10.1029/2002JD003290, in press, 2003b.

Cantrell, C. A., et al., Peroxy radical behavior during TRACE-P as measured aboard the NASA P-3B aircraft, *J. Geophys. Res.*, *108*(D20), 8797, doi:10.1029/2002JD003674, in press, 2003.

Chameides, W. L., and D. D. Davis, The free radical chemistry of cloud droplets and its impact upon the composition of rain, *J. Geophys. Res.*, *87*, 4863–4877, 1982.

Chameides, W. L., and J. C. G. Walker, A photochemical theory of tropospheric ozone, *J. Geophys. Res.*, *78*, 8751–8760, 1973.

Chameides, W. L., D. D. Davis, J. D. Bradshaw, M. O. Rodgers, S. T. Sandholm, G. Sachse, G. Gregory, and R. Rasmussen, Net ozone production over the eastern and central North Pacific as inferred from GTE/CITE 1 observations during the Fall, 1983, *J. Geophys. Res.*, *92*, 2131–2152, 1987.

Chen, G., et al., An assessment of HO_x chemistry in the tropical Pacific boundary layer: Comparison of observations with model simulations during PEM Tropics A, *J. Atmos. Chem.*, *38*, 317–344, 2001.

Crawford, J. H., et al., An assessment of ozone photochemistry in the extratropical western, North Pacific: Impact of continental outflow during the late winter/earlier spring, *J. Geophys. Res.*, *102*, 28,469–28,487, 1997a.

Crawford, J. H., et al., Implications of large scale shifts in tropospheric NO_x levels in the remote tropical Pacific, *J. Geophys. Res.*, *102*, 28,447–28,468, 1997b.

Crawford, J., et al., Assessment of upper tropospheric HO_x sources over the tropical Pacific based on NASA GTE/PEM data: Net effect on HO_x and other photochemical parameters, *J. Geophys. Res.*, *104*, 16,255–16,273, 1999.

Crutzen, P. J., A discussion of the chemistry of some minor constituents in the stratosphere and troposphere, *Pure Appl. Geophys.*, *106–108*, 1385–1399, 1973.

Danielsen, E. F., Stratosphere-troposphere exchange based on radioactivity, ozone and potential vorticity, *J. Atmos. Sci.*, *25*, 502–518, 1968.

Davis, D. D., et al., Photostationary state analysis of the NO_2-NO system based on airborne observations from the subtropical/tropical North and South Atlantic, *J. Geophys. Res.*, *98*, 23,501–23,523, 1993.

Davis, D. D., et al., Assessment of the ozone photochemistry tendency in the western North Pacific as inferred from PEM-West A observations during the fall of 1991, *J. Geophys. Res.*, *101*, 2111–2134, 1996.

Davis, D. D., et al., Marine latitude/altitude OH distributions: Comparison of Pacific Ocean observations with models, *J. Geophys. Res.*, *106*, 32,691–32,708, 2001.

DeMore, W. B., S. P. Sander, D. M. Golden, R. F. Hampson, M. J. Kurylo, C. J. Howard, A. R. Ravishankara, C. E. Kolb, and M. J. Molina, Chemical kinetics and photochemical data for use in stratospheric modeling, *JPL Publ. 97-4*, Jet Propul. Lab., Pasadena, Calif., 1997.

Gidel, L. T., and M. A. Shapiro, General circulation model estimates of the net vertical flux of ozone in the lower stratosphere and the implications for the tropospheric ozone budget, *J. Geophys. Res.*, *85*, 4049–4058, 1980.

Hoell, J. M., Jr., D. D. Davis, S. C. Liu, R. E. Newell, H. Akimoto, R. J. McNeal, and R. J. Bendura, Pacific Exploratory Mission-West (PEM-West B): February–March, 1994, *J. Geophys. Res.*, *102*, 28,223–28,239, 1997.

Jacob, D. J., J. A. Logan, and P. P. Murti, Effect of rising Asian emissions on surface ozone in the United States, *Geophys. Res. Lett.*, *26*, 2175–2178, 1999.

Jaffe, D., T. Anderson, D. Covert, R. Kotchenruther, B. Trost, J. Danielson, W. Simpson, T. Berntsen, S. Karlsdottir, D. Blake, J. Harris, G. Carmichael, and I. Uno, Transport of Asian air pollution to North America, *Geophys. Res. Lett.*, *26*, 711–714, 1999.

Kumar, P. P., G. K. Manohar, and S. S. Kandalgaonkar, Global distribution of nitric oxide produced by lightning and its seasonal variation, *J. Geophys. Res.*, *100*, 11,203–11,208, 1995.

Lefer, B., R. Shetter, S. Hall, J. Crawford, and J. Olson, Impact of clouds and aerosols on photolysis frequencies and photochemistry during TRACE-P: 1. Analysis using radiative transfer and photochemical box models, *J. Geophys. Res.*, *108*(D21), 8821, doi:10.1029/2002JD003171, in press, 2003.

Lelieveld, J., and F. J. Dentener, What controls tropospheric ozone?, *J. Geophys. Res.*, *105*, 3531–3551, 2000.

Levy, H., II, W. J. Moxim, and P. S. Kasibhatla, A global three-dimensional time-dependent lightning source of tropospheric NO_x, *J. Geophys. Res.*, *101*, 22,911–22,922, 1996.

Liu, H., D. Jacob, L. Chan, S. Oltmans, I. Bey, R. Yantosca, J. Harris, B. Duncan, and R. Martin, Sources of tropospheric ozone along the Asian Pacific Rim: An analysis of ozonesonde observations, *J. Geophys. Res.*, *107*(D21), 4573, doi:10.1029/2001JD002005, 2002.

Liu, S., D. Kley, M. McFarland, J. D. Mahlman, and H. Levy II, On the origin of tropospheric ozone, *J. Geophys. Res.*, *85*, 7546–7552, 1980.

Liu, S., et al., Model study of tropospheric trace species distributions during PEM-West A, *J. Geophys. Res.*, *101*, 2073–2085, 1996.

Logan, J. A., M. J. Prather, S. C. Wofsy, and M. B. McElroy, Tropospheric chemistry: A global perspective, *J. Geophys. Res.*, *86*, 7210–7254, 1981.

Lurmann, F. W., A. C. Lloyd, and R. Atkinson, A chemical mechanism for use in long-range transport/acid deposition computer modeling, *J. Geophys. Res.*, *91*, 10,905–10,936, 1986.

Madronich, S., and S. Flocke, The role of solar radiation in atmospheric chemistry, in *Handbook of Environmental Chemistry*, edited by P. Boule, pp. 1–26, Springer-Verlag, New York, 1998.

Mahlman, J. D., H. Levy II, and W. J. Moxim, Three-dimensional tracer structure and behavior as simulated in two ozone precursor experiments, *J. Atmos. Sci.*, *37*, 655–685, 1980.

Newell, R., and M. Evans, Seasonal changes in pollutant transport to the North Pacific: The relative importance of Asian and European sources, *Geophys. Res. Lett.*, *27*, 2509–2512, 2000.

Pickering, K. E., A. M. Thompson, R. R. Dickson, W. T. Luke, D. A. McNamara, J. P. Greenberg, and P. R. Zimmerman, Model calculations of tropospheric ozone production potential following observed convective events, *J. Geophys. Res.*, *95*, 14,049–14,062, 1990.

Pickering, K. E., A. M. Thompson, W.-K. Tao, and T. L. Kucsera, Upper tropospheric ozone production following mesoscale convection during STEP/EMEX, *J. Geophys. Res.*, *98*, 8737–8749, 1993.

Streets, D. G., T. C. Bond, G. R. Carmichael, S. D. Fernandes, Q. Fu, D. He, Z. Klimont, S. M. Nelson, N. Y. Tsai, M. Q. Wang, J.-H. Woo, and K. F. Yarber, An inventory of gaseous and primary aerosol emissions in Asia in the year 2000, *J. Geophys. Res.*, *108*(D21), 8809, doi:10.1029/2002JD003093, in press, 2003.

Talukdar, R. K., C. A. Longfellow, M. K. Gilles, and A. R. Ravishankara, Quantum yields of $O(^1D)$ in the photolysis of ozone between 289 and 329 nm as a function of temperature, *Geophys. Res. Lett.*, *25*, 143–146, 1998.

Thompson, A. M., and R. J. Cicerone, Possible perturbations to atmospheric CO, CH4, and OH, *J. Geophys. Res.*, *91*, 10,853–10,864, 1986.

Wang, Y. H., D. J. Jacob, and J. A. Logan, Global simulation of tropospheric O_3-NO_x-hydrocarbon chemistry: 1. Model formulation, *J. Geophys. Res.*, *103*, 10,713–10,725, 1998.

Wang, Y., et al., Intercontinental transport of pollution manifested in the variability and seasonal trend of springtime O_3 at northern middle and high latitudes, *J. Geophys. Res.*, *108*, doi:10.1029/2003JD003592, in press, 2003.

Wild, O., J. K. Sundet, M. J. Prather, I. S. A. Isaken, H. Akimoto, E. V. Browell, and S. J. Oltmans, CTM ozone simulations for the spring 2001 over the western Pacific: Comparisons with TRACE-P lidar, ozonesondes, and TOMS columns, *J. Geophys. Res.*, *108*(D21), 8826, doi:10.1029/2002JD003283, in press, 2003.

B. E. Anderson, M. A. Avery, J. D. Barrick, E. V. Browell, J. H. Crawford, M. A. Fenn, W. B. Grant, C. H. Hudgins, and G. W. Sachse, NASA Langley Research Center, Hampton, VA 23681, USA. (b.e.

anderson@larc.nasa.gov; m.a.avery@larc.nasa.gov; j.d.barrick@larc.nasa.gov; e.v.browell@larc.nasa.gov; j.h.crawford@larc.nasa.gov; m.a.fenn@larc.nasa.gov; w.b.grant@larc.nasa.gov; c.h.hudgins@larc.nasa.gov; g.w.sachse@larc.nasa.gov)

D. R. Blake and N. Blake, Department of Chemistry, University of California, Irvine, Irvine, CA 92697, USA. (drblake@uci.edu; nblake@uci.edu)

G. Chen, D. M. Cunnold, D. D. Davis, B. DiNunno, P. Jing, S. T. Sandholm, and D. Tan, School of Earth and Amospheric Sciences, ES&T Building, Georgia Institute of Technology, Atlanta, GA 30332, USA. (gao.chen@eas.gatech.edu; cunnold@eas.gatech.edu; douglas.davis@eas.gatech.edu; bdinunno@eas.gatech.edu; pjing@eas.gatech.edu; scott.sandholm@eas.gatech.edu)

B. G. Heikes, Graduate School of Oceanography, University of Rhode Island, Narragansett, RI 02882, USA. (zagar@notos.gso.uri.edu)

B. Lefer and R. E. Shetter, National Center for Atmospheric Research, 1850 Table Mesa Drive, P. O. Box 3000, Boulder, CO 80303, USA. (lefer@ucar.edu; shetter@ucar.edu)

S. Liu, Institute of Earth Sciences, Academia Sinica, Taipei, Taiwan 11529, ROC. (shawliu@earth.sinica.edu.tw)

S. Oltmans, National Oceanographic and Atmospheric Administration, Boulder, CO 80303, USA. (soltmans@cmdl.noaa.gov)

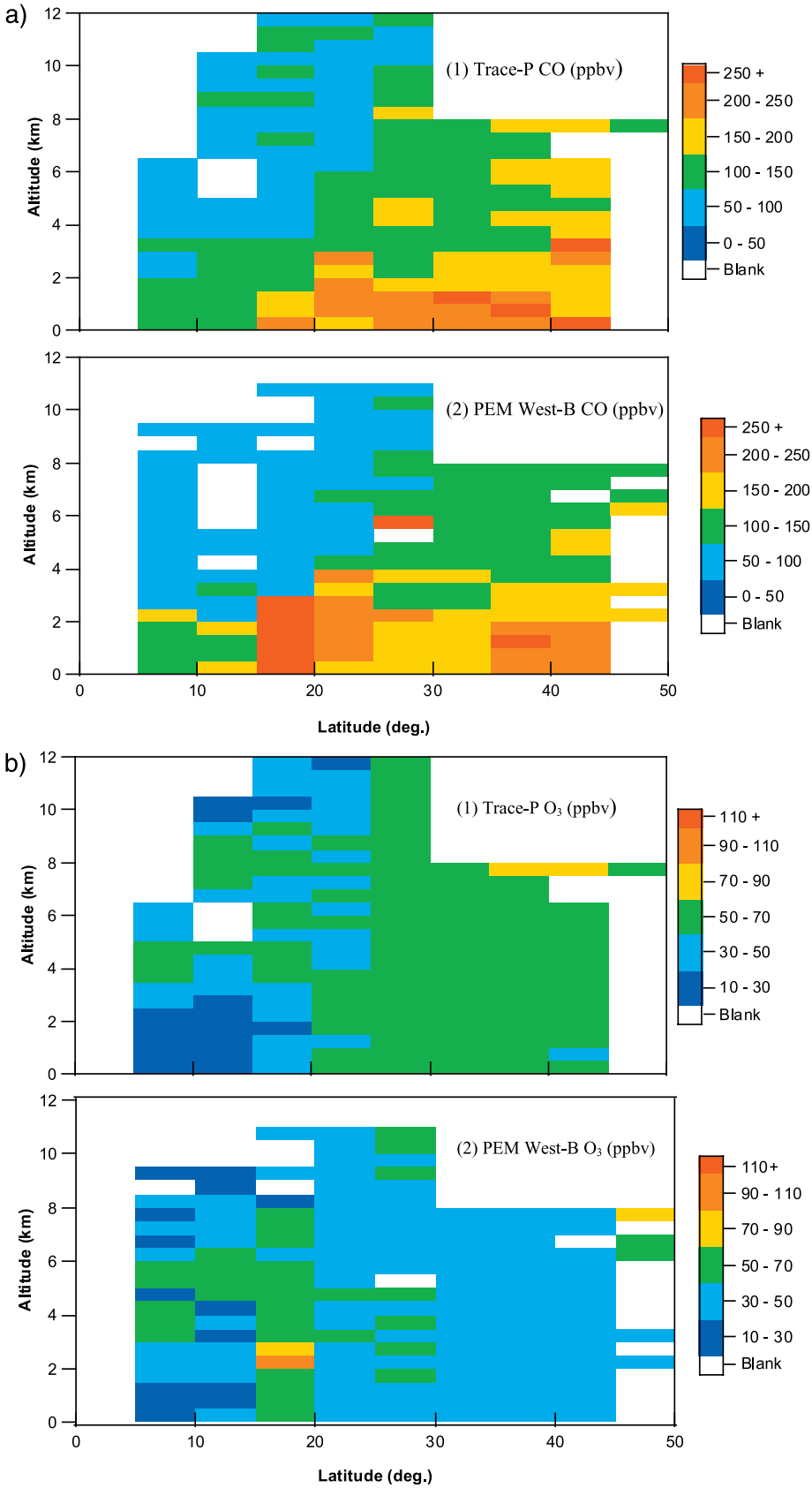

Figure 2. Altitude/latitude grid plots for (a) CO and (b) O_3. Panel 1 shows the observations from TRACE-P; panel 2 shows the observations from PEM-West B. Median values shown were estimated for each grid box, 0.5 km by 5° in size.

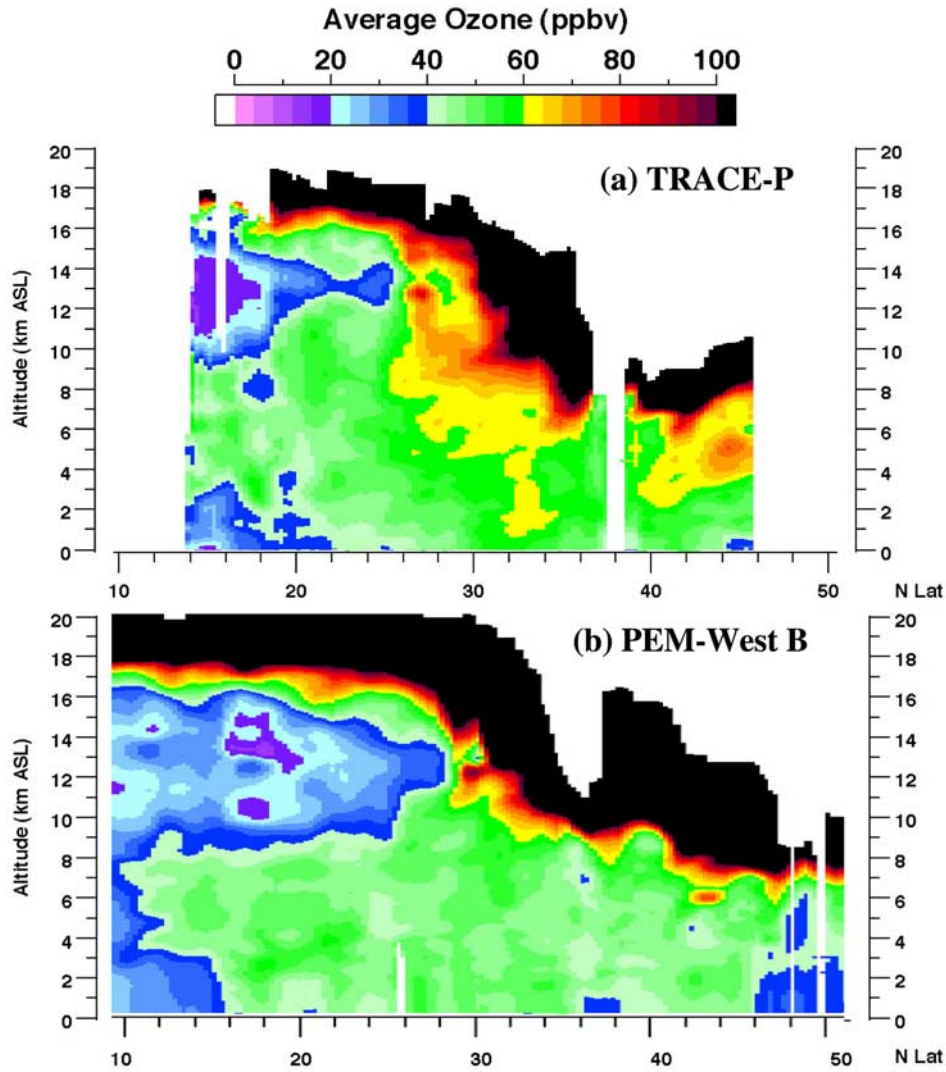

Figure 3. DIAL (Differential Absorption Lidar) O_3 observations as a function of altitude and latitude as observed during TRACE P (a) and PEM-West B (b).